LISBOA
UNIVERSIDADE DE LISBOA

FACULDADE DE MEDICINA LISBOA

TRABALHO FINAL
MESTRADO INTEGRADO EM MEDICINA

Oncobiologia

LDL favours metastatic spread of triple negative breast cancer

Miguel Esteves de Oliveira Santos

JUL'2019

LISBOA
UNIVERSIDADE DE LISBOA

FACULDADE DE MEDICINA LISBOA

TRABALHO FINAL
MESTRADO INTEGRADO EM MEDICINA

Oncobiologia

LDL favours metastatic spread of triple negative breast cancer

Miguel Esteves de Oliveira Santos

Orientado por:

Prof. Sérgio Dias

Prof. Sandrina Pereira

JUL'2019

ABSTRACT

Background: Breast cancer (BC) is the leading cause of cancer related death in women worldwide and metastasis account for the majority of mortality. Particularly, triple negative breast cancer (TNBC) has remarkably poor prognosis when metastasis develop. Dyslipidemia and mitochondrial adaptations have been implicated in metastatic progression. In this study, we explore the role of LDL and mitochondria in TNBC invasion-metastasis cascade, aiming at identifying new targets and prognostic markers that impact clinical management.

Methods: MDA-MB-231 human TNBC cell line was cultured in normal growth medium or supplemented with LDL. DiI-labelled-MDA-MB-231 (control) or Cy5-labelled-MBA-231 (LDL) cells transfected with Mito-YFP were xenotransplanted into the perivitelline sac of 2 days-postfertilization (pdf) zebrafish larvae. After injection, larvae at 1, 4, 5 days pos-injection (dpi) were fixed, stained for GFP and mounted. Tropism was studied using widefield and spinning disk confocal acquisitions. Mitochondrial network quantification was analysed with point scanning confocal images. Fisher Test, and chi-square, chi-square only and student T-test were applied for statistical analysis and p-values<0.05 were considered statistically significant.

Results: MDA-MB-231^{LDL} cells showed differential invasion potential (widefield analysis, Chi-square, p=0.0347, n=25 larvae; spinning disk analysis, Chi-square p=0.06, n=11 larvae), with cells disseminating to all organs in both analyses, contrary to MDA-MB-231^{control} cells. MDA-MB-231^{LDL} cells diverged from control and migrated more to less vascularised organs as well as exclusively infiltrated organs where no vessels are found at 6dpf. Mitochondrial network of disseminated MDA-MB-231^{LDL} cells had increased filamentous distribution across the cells, displaying more but smaller Mito-YFP particles, which according to literature is associated with migration and invasion.

Conclusions: Our results show that LDL exposure promotes invasion and survival of TNBC cells at distant sites and induce mitochondrial adaptations, i.e., increased mass, along with widespread of network across the cell, a metabolic feature with potential therapeutic application for metastatic TNBC.

Key-words: triple negative breast cancer, metastasis, LDL, mitochondria, zebrafish xenotransplantation

The Final Work does not express the opinion of FML, but only of the student.

RESUMO

O cancro da mama é o mais frequente entre mulheres em todo o mundo e é responsável pela maioria da mortalidade associada a cancro, no sexo feminino. As metástases são a principal causa de mortalidade, representando até 90% das mortes por cancro da mama.

O cancro da mama metastático tem mau prognóstico, embora haja diferenças significativas consoante o subtipo considerado. O cancro da mama triplo negativo metastático tem um tempo médio de sobrevida extraordinariamente inferior aos restantes, devido à ausência de receptores moleculares e terapêuticas dirigidas, à heterogeneidade molecular e à tendência para metastizar ou recidivar. A metastização ocorre segundo a cascata de invasão-metástase, que tem várias etapas: invasão local, intravasão, sobrevivência em circulação, extravasão, sobrevivência no microambiente secundário e proliferação para formar metástases. É imperativo compreender os mecanismos alterados na base da metastização do cancro de mama triplo negativo, isolar potenciais alvos terapêuticos e marcadores de prognóstico.

O LDL é uma lipoproteína de baixa densidade que transporta triglicéridos e colesterol esterificado do fígado para os tecidos periféricos. Níveis plasmáticos elevados de LDL estão associados a menor tempo livre de doença e maior progressão tumoral, em cancro de mama. A molécula de LDL tem impacto em várias etapas da cascata invasão-metástase. Destaca-se a promoção da perda de adesão à matriz, o aumento da invasão e migração, a estimulação de mecanismos que facilitam a intravasão e extravasão, bem como o aumento do número e tamanho de metástases pulmonares, em ratos hipercolesterolémicos, e nódulos linfáticos metastáticos, em pacientes com níveis plasmáticos de LDL aumentados. Nos carcinomas, a transição epitélio-mesenquimatosa está associada a facilidade em progredir na cascata metastática e o LDL induz a expressão de factores de transcrição que promovem este processo.

O metabolismo lipídico, em particular, altera-se substancialmente em tumores em progressão, como o triplo negativo. As células de cancro de mama triplo negativo têm alterações a vários níveis de regulação lipídica, aumentando o *uptake* de lípidos, facilitando o transporte intracelular de ácidos gordos e a activação necessária para armazenar lípidos em *lipid droplets* ou encaminhá-los para membranas lipídicas e para a oxidação de ácidos gordos. Além disso, apesar de serem globalmente mais glicolíticas, *subsets* de células triplo negativo têm demonstrado ser capazes de recorrer à utilização de oxidação de ácidos gordos e têm vários genes associados a esta via alterados. A elevada quantidade de energia providenciada por esta oxidação é vantajosa para a sobrevivência em

ambientes com nutrientes mais limitados, como em perda de adesão. De facto, a desregulação de alguns destes genes está associada a progressão metastática e a pior prognóstico em cancro triplo negativo. O microambiente tumoral no cancro da mama promove a progressão tumoral, contribuindo para a inflamação tumoral crónica (particularmente no caso da obesidade e dislipidemia), participa em permuta de metabolitos e fornece lípidos, que são transferidos para as células cancerígenas.

São conhecidas várias alterações mitocondriais, em células invasivas e metastáticas de cancro da mama, como a expressão e activação de proteínas associadas a fissão e biogénese mitocondrial. Como consequência, estas células têm uma rede mitocondrial com maior massa, mais fragmentada, e as mitocôndrias são transportadas para regiões distantes do núcleo, incluindo protusões citoplasmáticas, onde promovem a migração. Em circulação, estas células têm menor acesso a nutrientes, menor necessidade de captar substratos para metabolismo anabólico e maior necessidade energética, portanto o metabolismo energético é mais dependente da respiração mitocondrial e os genes associados à glicólise são sub-expressos.

Apesar de evidência recente sugerir que a exposição a LDL induz a agressividade de células TNBC ao modular a morfologia mitocondrial e o metabolismo, o mecanismo exacto destas alterações e as implicações para a progressão do cancro da mama, permanecem desconhecidos. Nesta dissertação, propusemo-nos estudar 1) se células de cancro da mama triplo-negativo após exposição a LDL têm um comportamento mais agressivo num organismo vivo, 2) se há invasão diferencial em órgãos secundários e 3) se as adaptações mitocondriais estariam correlacionadas com comportamento invasivo e tropismo diferencial. Para abordar estas questões, a linha celular humana de cancro da mama triplo negativo MDA-MB-231 foi cultivada em meio suplementado com LDL ou meio de crescimento normal. As células foram transfectadas com o marcador de mitocôndrias Mito-YFP, marcadas com DiI (MDA-MB-231controlo) ou com Cy5 (MDA-MB-231LDL), e xenotransplantadas em zebrafish com 2 dias pós-fertilização.

Aos 4 dias pós-injecção (6 dias pós-fertilização) a capacidade de células MDA-MB-231^{LDL} e MDA-MB-231^{control} migrarem para locais distantes em zebrafish foi analisada usando um microscópio *widefield*. De acordo com nossos resultados, células MDA-MB-231^{LDL} têm migração diferencial estatisticamente significativa em geral (Qui-quadrado p=0.0347) e particularmente para locais distantes, como barbata dorsal (teste de Fisher, p=0.042), músculo dorsal (p=0.05), notocorda (p=0.023) e barbatana anal (p=0.008). Contudo, como o sistema *widefield* apresenta algumas limitações, quantificámos a capacidade de invasão e colonização de células TNBC em *zebrafish* com

um sistema confocal *spinning disk*. Analogamente à análise anterior, os resultados revelaram uma tendência para migração diferencial em geral das células MDA-MB-231^{LDL} (Qui-quadrado, p=0.06, n=11). Estes resultados mostram ainda que células 1) MDA-MB-231^{LDL} são capazes de migrar para todos os órgãos analisados, ao contrário das MDA-MB-231^{control}; 2) órgãos mais vascularizados foram invadidos por células de ambas as condições, com as células MDA-MB-231^{control} a infiltrarem mais frequentemente zonas muito vascularizadas, especialmente CHT (teste de Fisher, p=0,02); 3) órgãos menos vascularizados foram invadidos preferencialmente pelas células MDA-MB-231^{LDL}. Entre estes, determinados órgãos são vascularizados apenas por uma artéria (olho, teste de Fisher, p=0,0075) ou eram justamente ventrais relativamente a CHT (barbatana anal) e foram invadidos pelo controle MDA-MB-231; mas outros (notocorda, barbatana ventral, barbatana dorsal, barbatana caudal) não têm vasos nos estudos angiográficos e nas nossas larvas Tg (*fli1: eGFP*) a 6dpf e foram exclusivamente infiltrados por células MDA-MB-231^{LDL}. Estes resultados sugerem que as células de ambas as condições são capazes de realizar os três primeiros passos da cascata invasão-metástase (invasão, intravasão, sobrevivência em circulação) mas a exposição a LDL acelera uma ou mais etapas da cascata metastática, facilitando a migração para áreas periféricas e não vascularizadas.

Interrogámo-nos porque é que as células MDA-MB-231^{LDL} têm propriedades migratórias aceleradas, mais invasivas ou menos dependentes da vascularização. Para compreender o panorama geral de migrações contámos as massas tumorais (clusters > 20 células) e as células disseminadas dentro do *zebrafish*, excluindo células em massas tumorais. Encontrámos uma maior proporção de células MDA-MB-231^{LDL} que células controlo no intestino (qui-quadrado, p<0,0001) e órgãos menos vascularizados: olho (Qui-quadrado, p<0,0001), músculo dorsal (Qui-quadrado, p=0,0336), notocorda (Qui-quadrado, p=0,0058), barbatana ventral (Qui-quadrado, p=0,0002) e barbata anal (Qui-quadrado, p=0,0236). As células MDA-MB-231^{control} acumulam-se de forma abundante em órgãos extremamente vascularizados - como vesícula óptica (Qui-quadrado, p=0,0073), coração (Qui-quadrado, p=0,0126), guelras (Qui-quadrado, p=0,0003) e CHT (Qui-quadrado, p<0,0001) e outras regiões que não atingiram significância estatística (PVS, fígado). Contudo, não foram detectadas células MDA-MB-231^{control} em regiões adjacentes não vascularizadas. Este fenótipo diverge do comportamento das células MDA-MB-231^{LDL} que apesar de serem encontradas em menor número e proporção nas regiões vascularizadas, conseguem migrar para as regiões sem vasos, como barbatana ventral, anal, dorsal, caudal e notocorda. A extravasão ou sobrevivência no microambiente distante parecem ser processos limitantes. Duas hipóteses podem explicar estes resultados: 1) quimioatracção das células MDA-MB-231^{control} especificamente para áreas vascularizadas; 2) aumento da agressividade das células MDA-MB-231^{LDL} dotadas de maior capacidade de

extravasamento ou sobrevivência fora do trânsito hematogénico ou ambos. Como as células partilham o mesmo microambiente, este quadro sugere que a extravasão e a sobrevivência à distância terão sido promovidas por transformações nas próprias células cancerígenas, induzidas pela exposição prévia a LDL. Colocamos como hipótese dois mecanismos adaptativos nas próprias células para explicar a alteração de comportamento após exposição a LDL: o desenvolvimento de *invadopodia* (protusões citoplasmáticas que promovem a extravasão) e utilização de oxidação de ácidos gordos (que aumenta a sobrevivência à distância). De facto, no início da experiência verificámos que a exposição a LDL nas células expostas aumentou o conteúdo de *lipid droplets* e pode ter sido utilizado para estes fins. Estudos futuros serão necessários para confirmar o aumento da FAO e de *invapodia* à distância nas células MDA-MB-231^{LDL}.

Massas de células tumorais (> 20 células) foram detectadas dentro dos órgãos previamente analisados e quantificadas. Os resultados mostram que MDA-MB-231^{LDL} foram capazes de crescer oito massas celulares tumorais e MDA-MB-231control foram capazes de crescer sete. De entre estes, contabilizaram-se cinco massas de células tumorais distantes para ambas as condições. Não houve diferença no número de massas distantes ou diferença relevante no número de massas globais.

Como a massa mitocondrial, a biogénese e a dinâmica foram previamente implicadas na aquisição de maior capacidade migratória, decidimos estudar o impacto do LDL na distribuição da rede mitocondrial, usando o sinal de Mito-YFP como marcação mitocondrial e recorrendo a microscopia confocal *point scanning*. A análise qualitativa de distribuição de rede mitocondrial mostrou que 54.7% das células MDA-MB-231^{LDL} adquirem uma distribuição filamentosa diferindo das células MDA-MB-231^{control} que maioritariamente têm uma distribuição perinuclear (Fisher Test, p=0.0429) Esta diferença advém das células MDA-MB-231^{LDL} que migraram (intestine, cérebro, *swim bladder*), é estatisticamente significativa no cérebro (p=0.0152), que revelou aumentou de tropismo e maior número de células MDA-MB-231^{LDL}. De acordo com a literatura, o transporte de mitocôndrias para a periferia do citoplasma é uma das alterações das células transformadas que confere propriedades invasivas e migratórias. Os resultados mostram que o LDL promove a aquisição de uma rede filamentosa, que é compatível com maior distribuição de mitocôndrias às periferias incluindo protusões citoplasmáticas.

Para estudar quantitativamente a rede mitocondrial, as imagens obtidas com o sistema confocal *point scanning* foram convertidas em projecções de máxima intensidade e os canais de Mito-YFP e DiI ou Cy5 foram processados como imagens binárias. Quantificámos o número de partículas Mito-YFP,

que representa a massa mitocondrial. Os resultados mostram um aumento generalizado do número de partículas Mito-YFP nas células MDA-MB-231 expostas a LDL em relação às controlo (Student T-test, $p<0.0001$), que foi estatisticamente significativo no PVS ($p=0.0304$), intestino ($p=0.0022$) e cérebro ($p=0.0456$), podendo assim concluir que a exposição a LDL induz um aumento de massa mitocondrial. Também quantificámos a área média de Mito-YFP por célula, uma medida de área de distribuição de rede mitocondrial na célula, que mostra um tendência para estar aumentada em células MDA-MB-231^{LDL} (Student T-test, $p=0.0723$), atingindo significância estatística no cérebro ($p=0.0237$) e na *swim bladder* ($p=0.0283$), o que sugere que a exposição a LDL promove o aumento da área de distribuição da rede mitocondrial. Por fim, quantificámos a área de Mito-YFP por partícula, que é uma medida indirecta do tamanho de cada mitocôndria. Os nossos resultados mostraram uma tendência para redução de área de Mito-YFP por partícula que apenas alcançou significância estatística no intestino (Student T-test, $p=0.0237$). Estes resultados sugerem que globalmente, o LDL parece induzir um aumento do número de mitocôndrias, embora com menor tamanho e uma maior área de distribuição da rede mitocondrial na célula. A literatura sugere que células tumorais em migração apresentam aumento de biogénese mitocondrial e fissão da rede e a exposição a LDL parece aumentar este fenótipo. O transporte de mitocôndrias para as protusões citoplasmáticas também aumenta as capacidades invasivas e migratórias. Curiosamente, a exposição a LDL aumentou da área de distribuição mitocondrial, o que se pode reflectir uma maior distribuição de mitocôndrias à periferia contribuindo para as características migratórias e invasivas das células MDA-MB-231.

Em suma, as células de cancro de mama triplo negativo estimuladas com LDL têm aumento de propriedades invasivas e migratórias em *zebrafish* xenotransplantados, que parecem estar associadas a transformações nas próprias células cancerígenas, que as terão dotado de maior capacidade de extravasão e sobrevivência à distância. O LDL induziu adaptações mitocondriais, nomeadamente disposição de rede filamentosa, aumento da massa mitocondrial, mas menor massa por mitocôndria. Estas transformações mitocondriais parecem ser um dos mecanismos pelos quais o LDL induz aumento de invasão, migração ou sobrevivência à distância nas células MDA-MB-231. Estudos futuros são necessários para confirmar estas hipóteses, nomeadamente o uso de larvas Tg (*fli1:eGFP*) xenotransplantadas separadamente com células MDA-MB-231^{LDL} ou MDA-MB-231^{control} com término da experiência a time-points posteriores (como 6 dpf) para avaliar o desenvolvimento de massas tumorais mais consideráveis, o tropismo, sobrevivência celular, rede mitocondrial e interacção das células com o endotélio. Ensaios que quantifiquem a utilização de oxidação de ácidos gordos pelas células TNBC e que clarifiquem a relação das mitocôndrias com as

protusões citoplasmáticas irão também ajudar a esclarecer o papel do metabolismo lipídico na agressividade das células TNBC. Elucidar estas questões será determinante para identificar alvos terapêuticos eficazes em cancro TNBC metastático, a fim de melhorar o *outcome* destas doentes.

Palavras-chave: cancro de mama triplo negativo, metástase, LDL, mitocôndria, xenotransplantação de zebrafish

O Trabalho Final exprime a opinião do autor e não da FML.

CONTENTS

List of figures

ACKNOWLEDGMENTS

To my grandmother Regina, who, through broad Talent, Fairness and Passion, paved the way and inspired my inner interest in Science since the beginning, I will always be grateful.

I am thankful for the chance to work in Sérgio Dias Lab, in Instituto de Medicina Molecular. As a medical student acknowledging the depth of the challenges cancer research faces has contributed to my development, for the awareness of the state of art and the need to bring contributions to this field. I am thankful to all the team, in particular to Patrícia, long hour coleague of lab and close tutor; to Sandrina, who shortened kilometres with relentless determination to support my work and always set the bar high in her corrections and accurate suggestions; to Sérgio, who took me into the team and into the work, enlightening our ideas and discussions. Thank you for the opportunity you provided me and the evolution you propelled.

Ana Nascimento, António Temudo, José Serrado Marques, José Rino, I thank you for sharing your knowledge in behalf of our experiments, for overcoming successive bioimaging challenges and solving doubts along the way.

To Professor Ruy Ribeiro, I am grateful for kindly receiving me and revising biostatistical issues regarding tropism analysis.

To Rita Fior for the zebrafish experiment, for suggestions, rectifications and confirmations.

To Jimite and Maia, for sharing days and nights of writing, for every discussion and suggestion. To all my friends along this six-year journey, and to those before, in particular Ibas.

To Francisco, Mom and Dad, for listening, revising, and being a privileged consultant team. For you always find time and space to be present, fuelling who I am. To all my family. Sincerely, thank you.

ABBREVIATIONS

ACACB – Acetyl-CoA carboxylase beta;

ASCL4 - Long-chain-fatty-acid—CoA ligase 4;

AKR1B10 - Aldo-keto reductase family 1 member B10;

Akt – Protein kinase B;

ATP - Adenosine triphosphate;

BC – Breast cancer;

BMI – Body mass index;

BSA - Bovine Serum Albumin;

CAT - carnitine acyl transferase;

CD36 – Cluster of differentiation 36;

CDCP1 - CUB domain-containing protein 1;

CHT – Caudal hematopoietic tissue;

CPT1- Carnitine palmitoyltransferase I;

CPT2 – Carnitine palmitoyltransferase II

DAPI - 4′,6-diamidino-2-phenylindole;

DMEM – Dulbecco's Modified Eagle Medium;

DMSO - Dimethyl Sulfoxide (DMSO);

dpf – days post fertilization;

dpi – days post injection;

Drp-1 – Dynamin related protein 1;

ECM – Extracellular matrix;

EMT- Epitelial-to-mesenchymal transition;

ER - Estrogen receptor;

ETC - Electron transport chain complex;

$FADH_2$ - Flavin adenine dinucleotide;

FAO – Fatty acid oxidation;

FABP – Fatty acid binding protein;

FBS – Fetal bovine serum;

FBS-LPF - Fetal bovine serum-lipoprotein free;

GFP – Green fluorescent protein;

HER2 - Human epidermal growth factor receptor;

HSP60 - Heat shock protein 60;

IGF-1 – Insulin growth factor 1;

LD – Lipid droplets;

LDL – Low-density lipoprotein;

LPL - lipoprotein lipase;

LPIN1 - Lipin 1;

MBC – Metastatic breast cancer;

Mfns – Mitofusins;

MS – Metabolic syndrome;

Myc – proto-oncogene Myc;

NADH - Nicotinamide adenine dinucleotide;

PBS – Phosphate-buffered saline;

PLA2G4- phospholipase A2, group IVA;

PFA – Para-formaldehyde ;

PGC-1α - Peroxisome proliferator-activated receptor-γ coactivator-1α ;

PR - progesterone receptor;

PVS – Perivitelline sac;

ROS – Reactive oxygen species;

RT – Room temperature;

Src - Proto-oncogene tyrosine-protein kinase Src;

SLUG – Transcription factor SNAI2;

SNAIL - Transcription factor SNAI1;

TCA- Citric acid cycle;

T-DM1 – Trastuzumab emtansine;

TN – Triple negative;

TNBC – Triple negative breast cancer;

TWIST1 – Transcription factor Twist-related protein 1;

VEGF – Vascular endothelial growth factor;

VLDLR – Very low density lipoprotein receptor;

ZEB1 – Transcription factor zinc finger E-box-binding homeobox 1;

1 INTRODUCTION

1.1 The impact of metastatic breast cancer

Metastatic breast cancer (MBC) is the leading cause of death amongst women with breast cancer (BC), being responsible for up to 90% of breast cancer related deaths,[1,2] As amongst women, BC is the most diagnosed cancer worldwide (2 088 849 cases in 2018) and the one which bears more deaths (626 679 in 2018), amongst women[3] metastasis are a major burden.

BC is considered metastatic if the disease has spread further than the breast and ipsilateral lymph nodes (axillary, internal mammary, infra and supraclavicular),[4] whether it is a *de novo* presentation (5% of patients) or a relapse after treatment (30% of patients).[5] At present, MBC is highly lethal and only 5% of patients achieve long-term disease control; median overall survival is set on 37.22 months and few therapeutic options with demonstrated survival benefit are available.[6]

Literature describes an improvement on MBC overall survival in the last 30 years related to new chemotherapy drugs, immunohistochemical intrinsic subtypes detection and directed therapies.[6,7] Since the studies of Perou and Sørlie,[8,9] clinical approach takes into account three different molecular BC subtypes based on multigene assay or immunohistochemical determination of estrogen receptor (ER), progesterone receptor (PR), human epidermal growth factor receptor 2 (HER2) status and ki-67: Luminal BC, including Luminal A (ER+ and/or PR+, HER2-, low Ki67) and Luminal B (ER+ and/or PR+, HER2-, high Ki67); HER2 BC, non-luminal (HER2+, ER- and PR-) or luminal (HER2+, ER+ and/or PR+) and Triple Negative (TN) BC (ER-/PR-/HER2-).[10] Median overall survival of Luminal MBC, HER2 MBC and TN MBC is respectively 42.12, 44.91 and 14.52 months, i.e., appears to be very subtype dependent.[6] In the last decades, improvements in MBC overall survival were ought to the advent of hormonal therapies, for Luminal BC (Aromatase Inhibitors and high-dose Fulvestrant); to anti-HER2 therapies (Trastuzumab, Pertuzumab, T-DM1, Lapatinib) and also to chemotherapy (Paclitaxel, Vinorelbine, Docetaxel, Capecitabine, Ixabepilone, Eribulin).[6,7] Other drugs were developed but no overall survival benefit was demonstrated.[6]

TNBC is the subtype with worse prognosis, accountable to an extremely aggressive clinical behaviour (high tendency to metastize and risk to relapse), molecular heterogeneity and lack of recognized molecular targets for therapy.[11,12,13]

Taking this into account, there is an urgent demand on shedding light on the mechanisms underlying the BC metastatic process, particularly on TN MBC. Tumours are now seen as clusters of neoplastic and stromal cells (recruited to create the microenvironment) that undergo phenotypic changes, the hallmarks of cancer. Metastasis is one of the hallmarks, consisting in the growth of new colonies in distant tissues.[14] The process that enables successful metastasis is called the invasion-metastasis cascade (Figure 1) and comprises 1) local invasion of primary tumour cells into surrounding tissues (loss of cellular adhesion, degradation of extracellular matrix (ECM) and migration through stroma), 2) intravasation to the circulatory system, 3) survival during hematogenous transit, 4) arrest and 5) extravasation, 6) survival in foreign microenvironments and 7) proliferation into the development of detectable metastatic lesions.[15,16,17,18] Identifying new prognostic and therapeutic targets throughout this process is necessary to effectively prevent and treat MBC.[19]

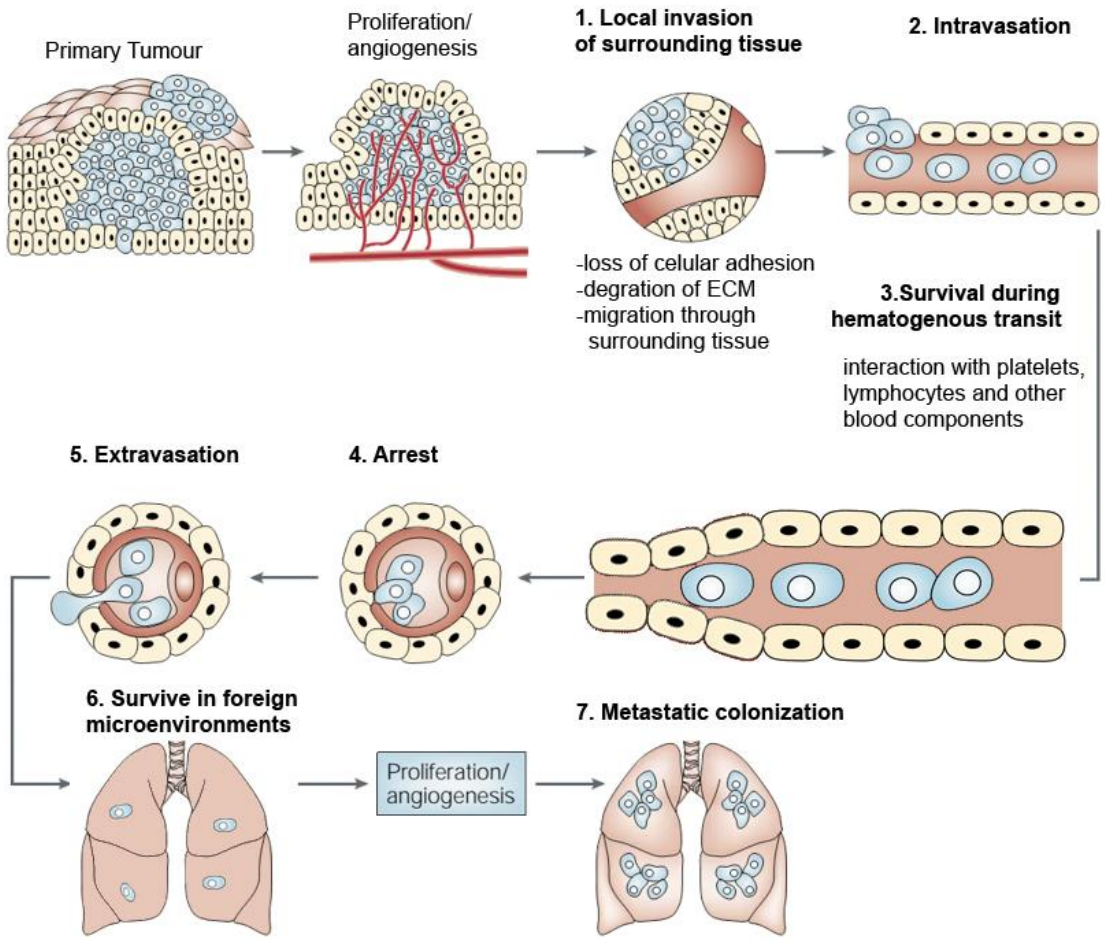

Figure 1: Invasion-Metastasis Cascade. Metastasis is a product of a serious of cell-events, to exit the primary site (1. detachment of primary site and invasion of surrounding tissues, 2. intravasate vessels), migrate systemically (3. survival on circulation, 4. arrest at a distant organ, 5. extravasate) and adapt to survive and thrive in that organ (6. survive in foreign microenvironments and 7. metastatic colonization). Carcinoma cells are depicted in blue. Adapted from [15,17].

1.2 LDL role on promoting metastatic TNBC

Diabetes, obesity and overweight have increased their prevalence over the last decades, worldwide.[20,21] Alarmingly, risk for BC raises in diabetic, obese and overweight postmenopausal women (and obese or overweight premenopausal women for TNBC). Outcomes in these BC patients were also poorer than normoglycemic or normal BMI patients.[22,23,24,25] Moreover, metabolic syndrome (MS) seems to aggravate even more BC prognostic since combined obesity and diabetes (2 out of 3 necessary criteria for MS) were independently associated with reduced disease-free survival and three-fold higher risk of BC recurrence.[26,27] Several mechanisms were proposed to explain the aggressive phenotypes, including chronic proinflammatory state; insulin-resistance, hyperinsulinemia and increased bioavailability of IGF-1; aromatase-driven estrogen production and increased estrogen levels due to decreased sex hormone binding protein; and altered cholesterol metabolism.[26,27,28,29]

Indeed, one of the targets under investigation concerning BC is low-density lipropotein (LDL). LDL is a lipoprotein with a core of triglycerides and cholesteryl esters and a surface monolayer with phospholipids and apoB-100 molecule[30] that generally carries cholesterol and triglycerides from liver to peripheral tissues.[31] LDL components seem to play important roles in BC: cholesterol is a component of cell membranes, where it wields structural functions and acts as a platform for signalling molecules in lipid rafts;[32] triglycerides may also be implied in metastatic BC metabolism. Higher LDL plasma levels have been linked to worse outcomes in BC patients (disease-free survival lowers)[33,34] and a role for cholesterol promoting BC progression seems to be setting up, with clinical data (higher LDL patients had larger, higher proliferative tumours and are more prone to LVI and lymph node metastasis)[33] and animal models evidence (hypercholesterolemic mice showed accelerated tumour formation and higher frequency of metastasis).[31,35]

LDL role over metastasis as a whole and in specific steps is quite documented. Revisiting the invasion-metastasis cascade, this lipoprotein may be involved in several steps of BC metastatic cascade.

Local invasion is promoted through loss of adhesion, degradation of extracellular matrix (ECM) and increased migration. Adhesion genes were down regulated and adhesion to matrix reduced in TNBC cell lines upon exposure to LDL.[31] BC cells invasion is fostered by the development of several cytoplasmatic protrusions: invadopodia[36] and lamellipodia[37]. ECM degradation is performed by invadopodium, ventral protrusions with lipid rafts where metalloproteinases (MT1-MMP) accumulate and focally degrade ECM, making a path for cells to migrate.[38,39] These protrusions are enriched in cholesterol and may not form in its absence.[40] Also, TNBC have high capability to

uptake LDL, store cholesterol and fatty acids in lipid droplets (LD), which are trafficked to cytoplasmatic protrusions, attached to microtubules.[41] Migration is also enhanced in TNBC cells exposed to LDL.[31,41] Chemoattracted-induced migration through the ECM in these cells relies on lamellipodium extensions protruding from the leading edge of the cell.[39,42] LDL exposure[31,41] and LD accumulation in these cytoplasmatic protrusions seem to also play a role increasing migration.[41]

Intravasion and extravasion of cancer cells require disruption of endothelial barrier so cells can cross the endothelium, a process named transendothelial migration.[43,44] Intravasation may be increased by high levels of LDL in 2 ways: it stimulates angiogenesis, creating new vessels with weaker cell-to-cell adhesions that allow easier intravasion;[35,45] and increases microenvironment inflammation, recruiting and stimulating macrophages activation, which facilitate intravasation.[29,44] In fact, intravasation in mice mammary tumour model occurs mostly in leaky vessels where perivascular macrophages are seen.[46]

Cell survival is increased upon LDL stimuli by the activation of Akt, in BC cell lines and murine models.[31,47,48] This survival pathway activates mechanisms that favour stress-induced apoptosis resistance.[49]

Differential arrest and extravasation of BC cells upon LDL exposure is mediated by one common mechanism: the increased microenvironment inflammation. Immune cells are recruited interacting with cancer cells, and most of these interactions increase cancer cells adhesion and extravasation.[29,44] In hypercholesterolemic mice, monocytes and macrophages are shown to adhere more to endothelium[45] and coincidently these myeloid cells were shown to promote extravasation in breast cancer, either secreting VEGF (thereby opening endothelial-cell junctions) or by increasing cancer cell survival.[44] Extravasation may also be promoted by providing cholesterol to invadopodia formation, which breach the endothelial junctions into the extravascular stroma;[50] as said before, invadopodia biogenesis may be halted in the absence of cholesterol plasma levels.[40,51]

Secondary growth at distance is endorsed by LDL since hyperlipidaemic $ApoE^{-/-}$ mice models have increased number and size of mammary metastasis in lungs[48] and patients with plasmatic LDL>144 mg/dL have increased number of lymph node metastasis.[33]

Some claim that dissemination of carcinoma cells are inducted into a process called epithelial-to-mesenchymal transition (EMT), which confers different adhesion molecules, motility, invasiveness and ability to degrade ECM - critical to invasion and metastasis.[18,52] Recently, a Systematic Review and Metanalysis of 3 218 MBC patients concluded EMT is critical for the acceleration of non-invasive to invasive BC and resistance to chemotherapy, and defined SLUG, TWIST1, SNAIL1,

ZEB1 as the key inducing transcription factors.[53] LDL may play a role in activating EMT[31] either directly, activating Akt,[54,49] or through cholesterol metabolite 27-OH.[29,55] Interestingly, MDA-MB-231 cells (TNBC line) exposed to LDL increased SLUG expression and EMT features; and inhibition of Akt decreased SLUG and EMT features.[54]

1.3 Mitochondrial metabolism in metastatic-TNBC

Mitochondria undergo changes that support cancer cells progression to metastasis.[56] To be exact, transformed mitochondrial function takes part in altered metabolism and energy production, regulation of calcium homeostasis, resistance to cell death programs, increased biosynthetic anabolism, increased ROS generation and acts as a hub for signalling pathways.[56]

Since mitochondrial morphology impact function, shape is tightly controlled by mitochondrial dynamics and is continuously changing.[57] Elongated filamentous networks result from fusion, i.e., merge of the outer and inner membranes of two or more mitochondria, regulated by Mfns1/2 and Opa1, respectively, and tend to occur either in quiescent cells, cells with large energy demands or cells in stress allowing increased ATP synthesis. Fragmented morphology is promoted by dynamin related protein 1 (Drp1), which regulates fragmentation so the energy-producing mitochondria can be redistributed to areas of greatest need of energy and damaged mitochondria can be degraded by mitophagy or autophagy.[57,58] Mitochondria may be distributed around the nucleus (perinuclear) or all around the cell (filamentous), depending on mitochondrial carriage by cytoskeleton to distant cellular destinations.[57]

In cancer cells, mitochondrial dynamics (Figure 2) enable local invasion and migration. Metastatic BC cells frequently overexpress Drp1 and downregulate MFN2, and as a result have fragmented mitochondria.[37] New evidence reinforces the hypothesis that hypoxia drives metabolic rewiring in BC cells, decreasing inhibitory phosphorylation of Drp1.[58] As a consequence, mitochondria undergo fission.[58] In fact, an analysis of human breast tissues demonstrated that mitochondria of invasive BC and metastasis on lymph nodes expressed significantly more Drp1 than carcinoma *in situ;* mitochondria of ductal carcinoma *in situ* expressed more Drp1 than normal breast tissue.[58] Also, active (phosphorylated) Drp1 was higher and mitochondria were more fragmented in metastatic cell lines (MDA-MB-231 and MDA-MB-436) than non-metastatic lines (MCF7).[58] In invasive and migrating cells, the formation of lamellipodia depends on fragmented mitochondrial network; after undergoing fission, mitochondria are shifted to lamellipodia[37] where ATP is highly needed to the

assembly of the cytoskeleton (F-actin).[37,58] Also, mitochondria control Ca^{2+} signals that regulate lamellipodia retraction and adhesion cycling, through the activation of actin filament contraction. Thus mitochondria effectively contribute to lamellipodia function: attaching to the substratum, contracting the trail rear edge and moving the cell toward lamellipodia.[59] Interestingly, assembly of actin, migration and invasion are impaired by mitochondrial fusion and high oligomycin A levels, an inhibitor of electron transport chain (ETC), suggesting that even though invasive and migrating cells depended on a fragmented mitochondrial morphology, they also rely on oxidative phosphorylation to migrate.[37]

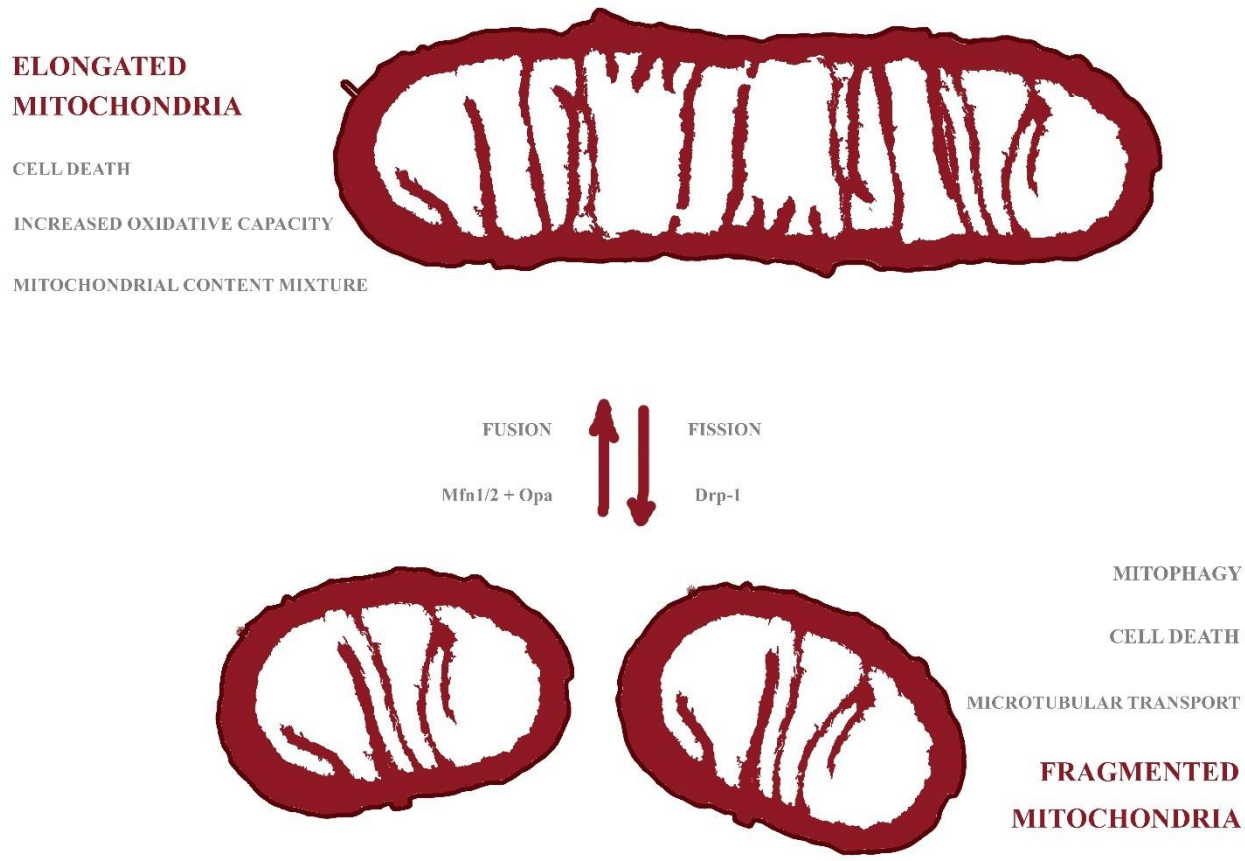

Figure 2: Mitochondrial dynamics. On top elongated mitochondria are represented with the processes related to it on the left. On the bottom fragmented mitochondria are represented with the processes related to it on the right. Arrows represent continuous mitochondrial dynamics, in which fusion promotes conversion of fragmented into elongated mitochondria through merge of inner and outter membranes regulated by Mitofusin1/2 (Mfn1/2) and Opa, respectively; fission promotes fragmentation of mitochondria through activation of Drp-1. Adapted from[58].

LeBleu *et al*. verified that circulating BC cells overexpress genes related with the typical EMT phenotype (*Snail1* and *Twist1*) along with oxidative phosphorylation, mitochondrial biogenesis and actin cytoskeleton signalling, compared to primary and secondary proliferating cells.[60] PGC-1α is an integrator of cellular signals regulating mitochondrial biogenesis, oxidative phosphorylation, fatty acid biosynthesis/oxidation and thermogenesis; the transcription of this protein regulator is increased in human circulating BC cells, particularly at the invasive tumour front and distant metastasis.[60] PGC-1α knockdown reduced mitochondrial biogenesis, oxidative phosphorylation, ATP-coupled oxygen consumption rate, migration and invasion in BC cell lines, in *in vitro* assays.[60] The same knockdown in BC cell lines xenotransplanted into mice reduced colonization and metastases formation, but had no effect on the growth of primary tumour.[60]

So, the pathways and substrates used throughout the invasion-metastasis cascade are different according to the bioavailability in the microenvironment and the metabolic needs of cancer cells. Proliferating cancer cells in primary or secondary site generally have more access to glucose and higher needs of metabolic intermediaries, and so engage on glycolysis even in aerobiosis (the Warburg effect) using glycolytic intermediaries to biosynthesize *de novo* nucleic acids, lipids and amino acids that support the unrestricted growth.[56,60,61] Migrating, invading and circulating tumour cells are quiescent and majorly engage on OXPHOS, which enables maximum energetic yield under poor access to nutrients and is important for the invasive properties of disseminating cells.[60]

1.4 FAO and mitochondrial metabolism driving metastatic TNBC

Dysregulation of lipid metabolism is a typical feature of progression in many types of cancers, including BC. Lipid metabolism comprises exogenous lipid uptake, *de novo* synthesis, activation, incorporation into glycerides, storage as triglycerides as well as cholesterol esters in lipid droplets, mobilization from phospholipids or triglycerides, and FAO.[62]

FAO is a metabolic pathway that generates large quantities of ATP through catabolism of fatty acids. Firstly, CPT1 conjugates fatty acids with carnitine to acylcarnitines and translocates them into the mitochondria. Then, in the mitochondrial matrix, a series of cyclical reactions cleave acylcarnitines to acetyl-CoA, generating NADH and $FADH_2$. Finally, acetyl CoA enters the tricarboxylic acid cycle (TCA), NADH and $FADH_2$ are shuttled to electron transport chain (ETC) to generate ATP.[63]

In TNBC several processes of lipid metabolism are dysregulated (Figure 3), including increased exogenous fatty acid and oxidized-LDL uptake due to upregulation of CD36[64,65] (among others)[62];

facilitated intracellular fatty acid transport by overexpression of transport proteins;[62] augmented activation of fatty acids,[62] i.e. esterification prior to FAO or synthesis of more complex lipids and subsequent elevated accumulation of cholesterol esters and triglycerides in LD.[62] Lipid droplets interact with a series of organelles and transfer lipids to membranes, to posttranslational modifications or fatty acid oxidation (FAO).[62]

Despite having a specifically high glycolytic profile manifested by increased glucose uptake, high lactate production, and decreased mitochondrial respiration,[66,67] TNBC can opt to use FAO under favourable microenvironment conditions.[62,68,69] FAO in TNBC provides survival advantage in nutrient deprived conditions,[62,68,69] such as loss of attachment to extracellular matrix.[63,68,70] This ability is advantageous as this alternative pathway is extremely energetic (renders more ATP per molecule metabolized), meeting migrating cells high energy demands to scape anoikis-cell death in circulation and face survival challenges in secondary site.[63,69] TNBC subset have FAO enzymes upregulated,[71,72] increased ETC activity by Src;[72] some cells overexpress Myc,[68] AKR1B10[69] or PML,[70] regulators of FAO-related enzymes.

Some of these alterations are associated with metastatic progression[69,73] and worst prognosis[69,70,71,] in human cancers including TNBC, including upregulation of fatty acid uptake (CD36 expression[65] and others[62]), fatty acid oxidation related genes (including CPT1C),[73] or decreased expression of ACACB (CPT1A and CPT1B indirect downregulator),[68] AKR1B10[69] or PML[70], supporting a role for lipid uptake and metabolism in metastatic progression,

Also, as mentioned before, tumours are clusters of neoplastic and tumour activated stromal cells.[14] The crosstalk between these plays an important role in initiating and maintaining TNBC invasion-metastatic cascade. Breast stromal cells include adipocytes, adaptative immune cells and mesenchymal stromal cells; collectively they are implicated in cancer progression.[74,75] Breast adipocytes, particularly, dedifferentiate into pre-adipocytes[76] or reprogram into cancer-associated adipocytes[76] and beyond playing a role in secreting cytokines (specially in obesity and dyslipidaemia), which increase chronic tumour-associated inflammation, engage in exchange of metabolites and provide a supply of lipids, which are transferred to cancer cells and fuel FAO or are used as structural lipids.[14,74,76]

In sum, metastatic potential and survival in circulation and at distance are favoured by a systemic set of adaptations that maximize TNBC cells ability to undertake FAO when necessary.

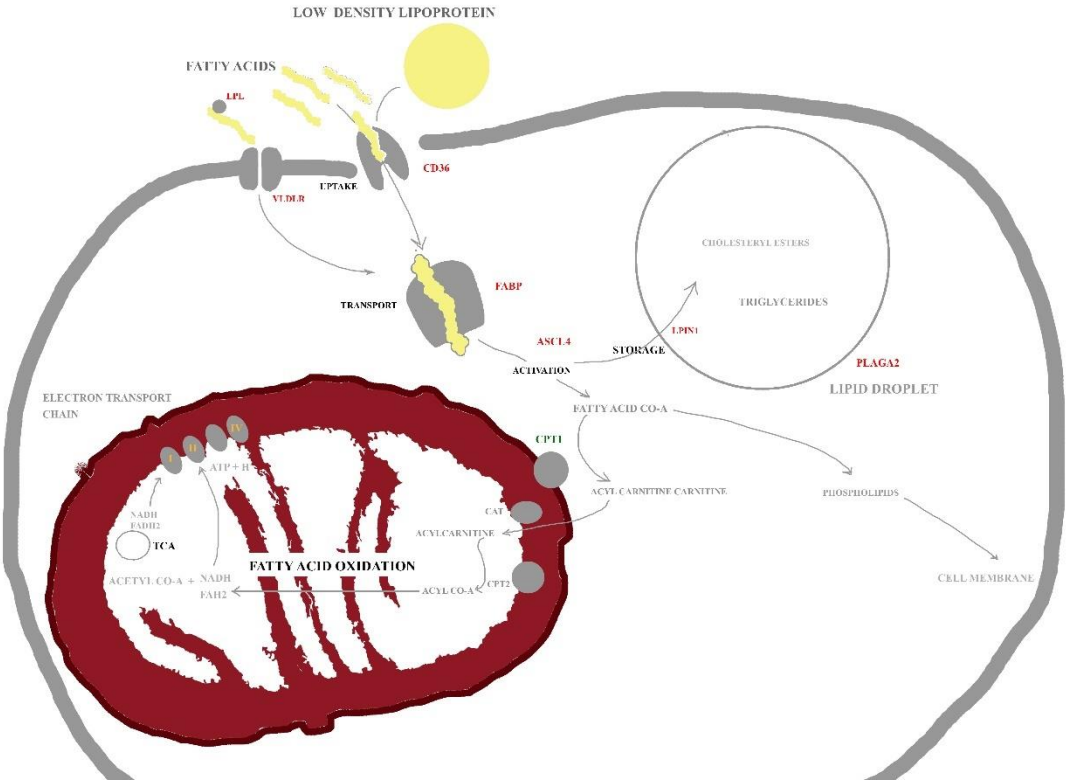

Figure 3: Lipid Metabolism. Red depicts proteins overexpressed in TNBC; orange represents proteins upregulated by increased phosphorylation; green depicts proteins with increased activity in TNBC. Low density lipoproteins and fatty acids are imported into the cell by CD36, or through other receptors including VLDLR. Fatty acids are activated, being directed to lipid droplets, mitochondria, phospholipids or exported. In the outter mitochondrial membrane CPT1 conjugates fatty acids with carnitines and transfers them to the mitochondria. CAT translocates acylcarnitines to mitochondrial matrix and CPT2 uncouples acylcarnitines to acyl CoA. Acyl CoA undergoes fatty acid oxidation, generating FADH2, NADH and Acetyl-CoA. NADH and FAH2 are transported to ETC, producing ATP. Acetyl-CoA may enter the Tricarboxylic Acid Chain (TCA), generating further NADH and $FADH_2$, that may be directed to the electron transport chain. ASCL4- Long-chain-fatty-acid-CoA ligase 4; CAT-carnitine acyl transferase gene; CPT1: Carnitine palmitoyltransferase I; CPT2- Carnitine palmitoyltransferase II; FABP – Fatty acid binding protein; LPIN1 –lipin-1; TCA - Citric acid cycle; PLA2G4 - Cytosolic phospholipase A2; VLDLR – very low density lipoprotein receptor. Adapted from[62,72,77]

1.5 Xenotransplanted zebrafish: an *in vivo* model to study BC metastasis

Cancer xenotransplantation is the implantation of cancer tumour cells or human cancer cell lines into an organism of other species.[78] Traditionally, murine models were used, but lately zebrafish (*Danio rerio*) has been used in the study of over 15 types of cancer.[79,80,81,82]

Zebrafish brings out new translational possibilities.[78] To start with, it allows studies to overcome ethical concerns related to cancer development and drug discovery.[78] As an animal model, *Danio rerio* is the only vertebrate system that allows whole organism detection of micrometastasis at a single cell level. Moreover, experiments can be carried out in transgenic fish, including whole-life

transparent *Danio rerio casper*, semi-transparent *nacre* or Tg (*fli1:eGFP*), which expresses GFP endothelial protein and can be used to track the invasion-metastasis cascade more accurately; or in wildtype zebrafish (transparent in the beginning of its life cycle).[78,83] Other advantages include shorter time frame experiments enable faster conclusions;[82] requiring less cancer cells (50-300) increases reproducibility and statistical significance of results;[78,84] lack adaptive immune system until 21 days post fertilization (dpf) makes immunosuppression unnecessary.[84,85]

To study metastasis generally Tg (*fli1:eGFP*) is recommended[78,85,86] at 48 hour post fertilization (hpf).[78,85,87] At this timepoint, passive diffusion effect is less probable to occur (since gastrulation is completed, body plan is mainly formed, organ systems are developed and vasculature is mapped), possible rejections are prevented, nutrition is granted by the large yolk, as well as safe injection of cells.[78] For cell analysis, live or fixed imaging at a laser scanning confocal microscope is recomended.[78,87] Interpretation of results must take into account the concept of migration, micrometastasis and tumour-like masses, where migration is defined as more than 5 cells outside the yolk sac and within the zebrafish[78,87], micrometastasis as the presence of daughter cells at 3 dpi and tumour cell masses are all clusters of more than 20 cells.[82]

Vascular system plays a role in human cancer dissemination.[18] Conviniently, zebrafish circulatory system is exhaustively studied, including at 2-6 dpf.[88] At 2 dpf (Figure 4A), the vascular system is already closed. Blood enters into the heart by the duct of Couvier, which directly drains the perivitelline sac and receives other tributaries; after, it is sent to the organism through aortic arches.

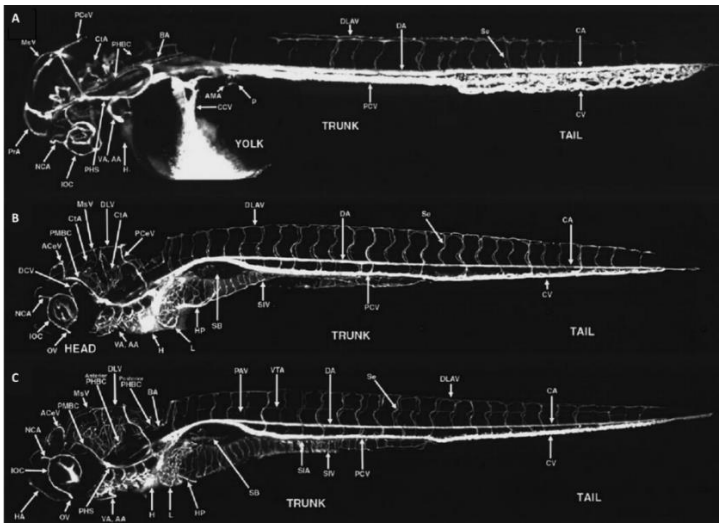

Figure 4: Circulatory system development of zebrafish larvae. A) Angiography of 2 dpf, larvae compiled by merging three separated reconstructions. B) Angiography of 5.5 dpf and C) 6.5 dpf larvae compiled by merging five separated reconstructions. Adapted from [88]

At 6 dpf (Figure 4B-C), zebrafish vascular system complixifies. Two (bilateral) arteries leave the heart and give colaterals to highly vascularised organs including gills, head kidney, liver, swim bladder, located in ventral head and trunk. Ventral trunk also includes intestine with considerable vascular supply. In the head, PICA takes blood to brain, forming a network. Eye is vascularised by a single peripheral artery, optic artery. Dorsal trunk and tail are vascularised by an axial system: blood is taken by dorsal aorta, in the trunk, and caudal artery, in the tail; caudal vein, in the tail, and posterior cardinal veins, in the trunk, bring blood. CHT, the plexus between caudal artery and caudal vein, is the more vascularised area of the tail. Intersegmented vessels cross transversally along muscles. Notochord is not pierced by vessels. Fins are vascularised in adulthood but no vessels are detected in angiographic studies at 6 dpf.[88]

1.6 Aim of the work

Recent in vitro work from our lab, suggests LDL might play its role in BC invasive properties through mitochondrial adaptations, with increase migration and mitochondrial mass in LDL-exposed BC cells (unpublished data). Despite this knowledge, the exact mechanisms that mediate LDL-induced aggressiveness in breast cancer progression remain unclear.

In this context, we decided to investigate whether 1) a more aggressive behaviour would also occur in LDL-exposed TNBC (MDA-MB-231) cells upon inoculation in a living organism, 2) if differential invasion to secondary organs would be observed (tropism) and 3) whether undergoing mitochondrial adaptations would be correlated to invasive behaviour and differential tropism.

2 MATERIALS AND METHODS

Cell culture

MDA-MB-231 human breast cancer cell line was cultured in DMEM (Thermo Fisher Scientific) supplemented with 10% (v/v) heat-inactivated FBS (Gibco Invitrogen) and 1% Antibiotic-Antimycotic (Gibco Invitrogen), named complete DMEM and incubated at 37ºC and 5% CO2 atmosphere.

At day 1, MDA-MB-231 cells were seeded at a density of $6x10^6$ (control) or $4,5x10^6$ (LDL) cells in a petri dish in complete DMEM and later (6h after), the medium was replaced by DMEM supplemented with 1% (v/v) FBS-LPF (fetal bovine serum-lipoprotein free) (Bio West). At day 2, the medium was replaced by fresh DMEM with 1% FBS-LPF alone or supplemented with LDL 100 µg/mL (Merck) for a total of 48h (until day 4). At day 3, cells were transfected with 6µg Mito-YFP using FuGENE (ThermoFisher Scientific) and according to the manufacturer instructions. At day4, MDA-MB-231 cells were detached with non-enzymatic methods (Cell Dissociation Buffer, enzyme-free, PBS; ThermoFisher Scientific) and stained separately with DiI (control) or Cy5 (LDL) (ThermoFisher Scientific) and subsequentially mixed before injected into zebrafish larvae (1:1 proportion at $0.5x10^6$ cells/ µl).

Flow cytometry

For lipid droplets quantification, cells were stained with BODIPY 493/503 (Molecular Probes; 0,2µg/mL) for 10 minutes at RT in the dark followed by analysis in a LSR Fortessa (BD Biosciences) flow cytometer and FlowJo software (LLC).

Zebrafish Xenograft injection

This experiment was performed in collaboration with Rita Fior and performed at Champalimaud Center for the Unknown. Zebrafish (*Danio rerio*) casper, nacre, and Tg (*fli1:eGFP*) fish were handled according to European animal welfare regulations and standard protocols. Mixed Cy5 (LDL) and DiI (control)-stained MDA-MB-231 cells were injected (mixed 50:50 at a concentration of $0.5x10^6$cel/µl) into the PVS of anesthetized 48-hpf larvae. After injection, xenografts were transferred to 34°C until the end of experiments. Larvae with cells in the yolk or cellular debris were discarded**.**

Zebrafish larvae whole mount immunofluorescence

Zebrafish larvae at 1, 4 and 5 days pos-injection (dpi) were fixed with 4%PFA (tebu-bio) and 0.1% Triton X-100 (Sigma) for 2h at RT and stored in MetOH 100% at -20ºC. In the first day, MetOH series were used to re-hydrate larvae. Larvae were washed twice for 5 min at RT in PBS1x and Triton X-100 0.1% and washed once with H2O. Larvae were incubated 7 min at -20ºC in Acetone and were washed with Glycine buffer (50ml PBS, 50 µl/mL Tween 20 (Sigma), 50 µl/mL Triton X-100 (Sigma), $7.5x10^{-3}$g/mL glycine (NZYtech) in PBS for 1h at 4C followed by washing with PBS 1x Triton X-100 0.1%. Larvae were blocked using PBDX_GS (50ml PBS, 0.01g/mL BSA (Sigma), 0.01ml/mL DMSO (Sigma), 5 µl/mL Triton X-100, 3 µl/mL goat serum (DAKO)) for 1h at RT. Primary mouse anti-human HSP60 antibody (BD Biosciences,1:50) was diluted in PBDX_GS buffer and incubated for 1h at RT followed by over-night at 4ºC. On the next day, larvae were rinsed twice with PBS1x Triton X-100 0.1% for 10 min at RT followed by four washes for 30 minutes at RT. Secondary donkey anti-mouse Alexa 488 (Invitrogen, 1:400) and rabbit anti-GFP made Alexa 488 (Invitrogen, 1:100) plus DAPI (1:200 from 20mg/ml stock; Millipore) were diluted in PBDX_GS buffer for 1h RT followed by over-night at 4ºC. On the following day, larvae were washed four times with PBS 1x Tween 20 0.05% for 15 minutes and fixed with 4%PFA for 20 minutes at RT, followed by five washed with PBS1x Tween 20 0.05% for 5 minutes at RT. Zebrafish larvae were mounted with mowiol mounting media.

Microscopy acquisition

Initial migration screening images of zebrafish larvae were acquired using inverted fluorescence widefield microscope Zeiss Axiovert 200M, with 10x amplification. Settings were defined with MetaMorph 7.8.0.0 software. For a more detailed tropism evaluation, tiles of zebrafish larvae were acquired using the spinning disk confocal microscope Zeiss Cell Observer SD, with 10x magnification. Settings were defined using ZEN 2.6 (blue edition). For mitochondrial network quantification it was used the inverted fluorescence microscope Zeiss LSM 880, with 63x Oil magnification, 1.6x zoom. Settings were defined with ZEN 2.1 (black edition).

Analysis of microscopic images and Statistics

Images were edited with (Fiji is Just) ImajeJ 2.0.0.[89] and the same settings were applied to images acquired with the same microscope. For the initial tropism study, the presence or absence of control cells (MDA-MB-231 cultured in a normal medium) and LDL-cells (MDA-MB-231 grown in

supplemented medium) in each organ was evaluated. Fisher Test was applied using GrafPadPrism 8.0.2, p-values <0.05 were considered statistically significant.

For the detailed tropism analysis regions of 6 dpf zebrafish were defined according to literature[68-73] and Fisher Test was applied using GrafPadPrism 8.0.2, p-values <0.05 were considered statistically significant.

For the quantification of the MDA-MB-231^{control} or MDA-MB-231^{LDL} cells per or organ, Imaris 9.0.1 was used. Tiles were converted into three-dimensional reconstructions, and cancer cells in each organ were quantified. Chi-square was applied to the data, p-values <0.05 were considered statistically significant.

For the qualitative analysis of mitochondrial distribution, the correspondent sub z-stack of each cell was produced. For the quantitative analysis, the channels correspondent to membrane dye and Mito-YFP of each sub z-stack were merged, converted to binary and the "Analyse particles" tool was used. Student T test was applied, p-values <0.05 were considered statistically significant.

3 RESULTS

3.1 Role of LDL in the invasion potential of TNBC cells in xenotransplanted zebrafish larvae using wide field fluorescence microscopy

We first analysed the ability of MDA-MB-231^{LDL} and MDA-MB-231^{control} cells to migrate to distant sites in zebrafish using widefield Zeiss Axiovert 200M microscope where the number of zebrafish larvae displaying MDA-MB-231 cells in several organs was evaluated (Figure 5).

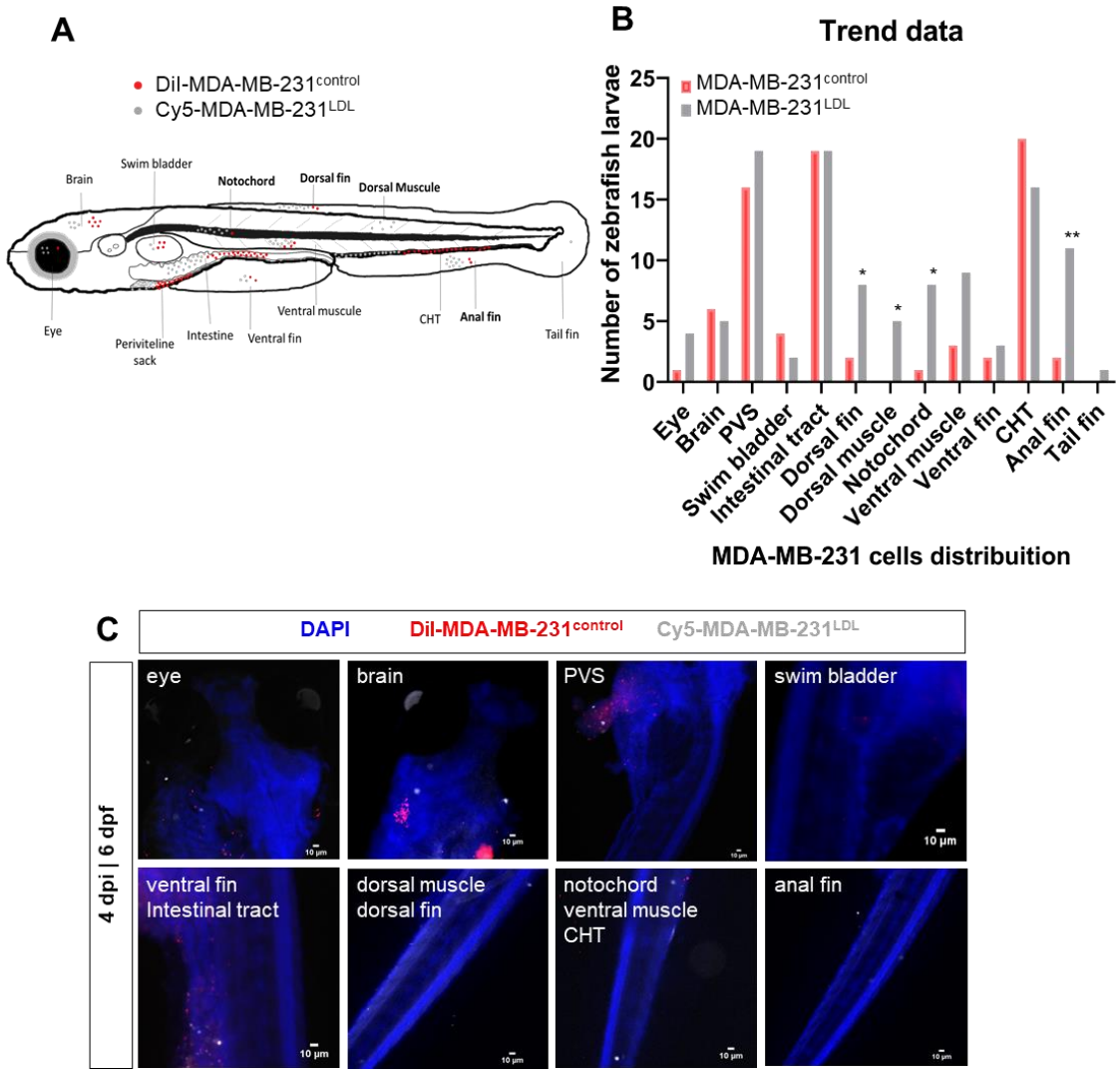

Figure 5:. TNBC MDA-MB-231 cells exposed to LDL show differential invasion potential to distant sites in xenotransplanted 4dpi zebrafish larvae.

A. Schematic representation of MDA-MB-231 cells invasion potential at 4dpi (6dpf) throughout the zebrafish body with DiI-labelled MDA-MB-231 control (red) and Cy5-labelled LDL-exposed (grey) cells detected in the indicated organs (bold depicts regions with increase tropism for LDL-exposed MDA-MB-231 cells), each dot represents one xenograft.[90,91,92]

B. Quantification of the invasive potential depicted as the number of zebrafish larvae xenografts (n=25 from 1 independent experiment) with DiI-labelled MDA-MB-231 control (red) and Cy5-labelled LDL-exposed (grey) cells in the indicated organs. Statistic significance was determined with the Fisher test.* $p<0.05$ and ** $p<0.01$.

C. Representative images of screened organs in zebrafish body (4dpi and 6dpf), including the eye, brain, perivitelline space (PVS), swim bladder, ventral fin and intestinal tract, dorsal muscle and fin, notochord, ventral muscle and caudal hematopoietic tissue (CHT) and anal fin, invaded by DiI-labelled MDA-MB-231 control (red) and Cy5-labelled LDL-exposed (grey) cells and captured with an inverted fluorescence widefield Zeiss Axiovert 200M. Nuclei staining with DAPI is in blue.

According to our results (Figure 5A and Supplementary Table1), MDA-MB-231^{LDL} have statistically significant differential migration in general (Chi-square p=0.0347) and particularly towards distant sites, such as dorsal fin (Fisher Test p=0.042), dorsal muscle (p=0.05), notochord (p=0.023) and anal fin (p=0.008). Moreover, dorsal muscle and tail fin were preferentially invaded only by MDA-MB-231^{LDL}.

Widefield acquisitions restrained us to evaluate whether cells were inside peripheral vessels or had already extravasated. Therefore, with these data we can only infer that LDL exposure favoured MDA-MB-231 cells with metastatic/more invasive abilities by accelerating or facilitating one or more steps of the metastatic cascade.

3.2 Role of LDL in the invasion potential of TNBC cells in xenotransplanted zebrafish larvae using inverted spinning disk confocal microscopy.

Widefield Zeiss Axiovert 200M is not the gold-standard bioimaging system to study zebrafish, according to literature.[78,79,80] On the one hand, it does not allow us to capture all the slices of zebrafish larvae thickness, preventing us to take full advantage of our *in vivo* model. On the other hand, the system is not able to capture a unique layer with accurate resolution, thus, some organs of the zebrafish (liver, head kidney, heart, gills and optic vesicle) had to be ruled out from the previous analysis.

In order to confirm the validity of our previous results, we quantified the invasion and colonization capability of TNBC cells in xenotransplanted zebrafish larvae using an inverted spinning disk Zeiss Cell Observer SD confocal (Figure 6). This technology allowed us to understand the full frame of migration in the whole organism and differential cell distribution by counting the number of cells in each organ. Moreover, we could access the colonization capability by inferring whether MDA-MB-231^{LDL} would be more successful in growing tumour cell masses (>20 cells) after migration.[82]

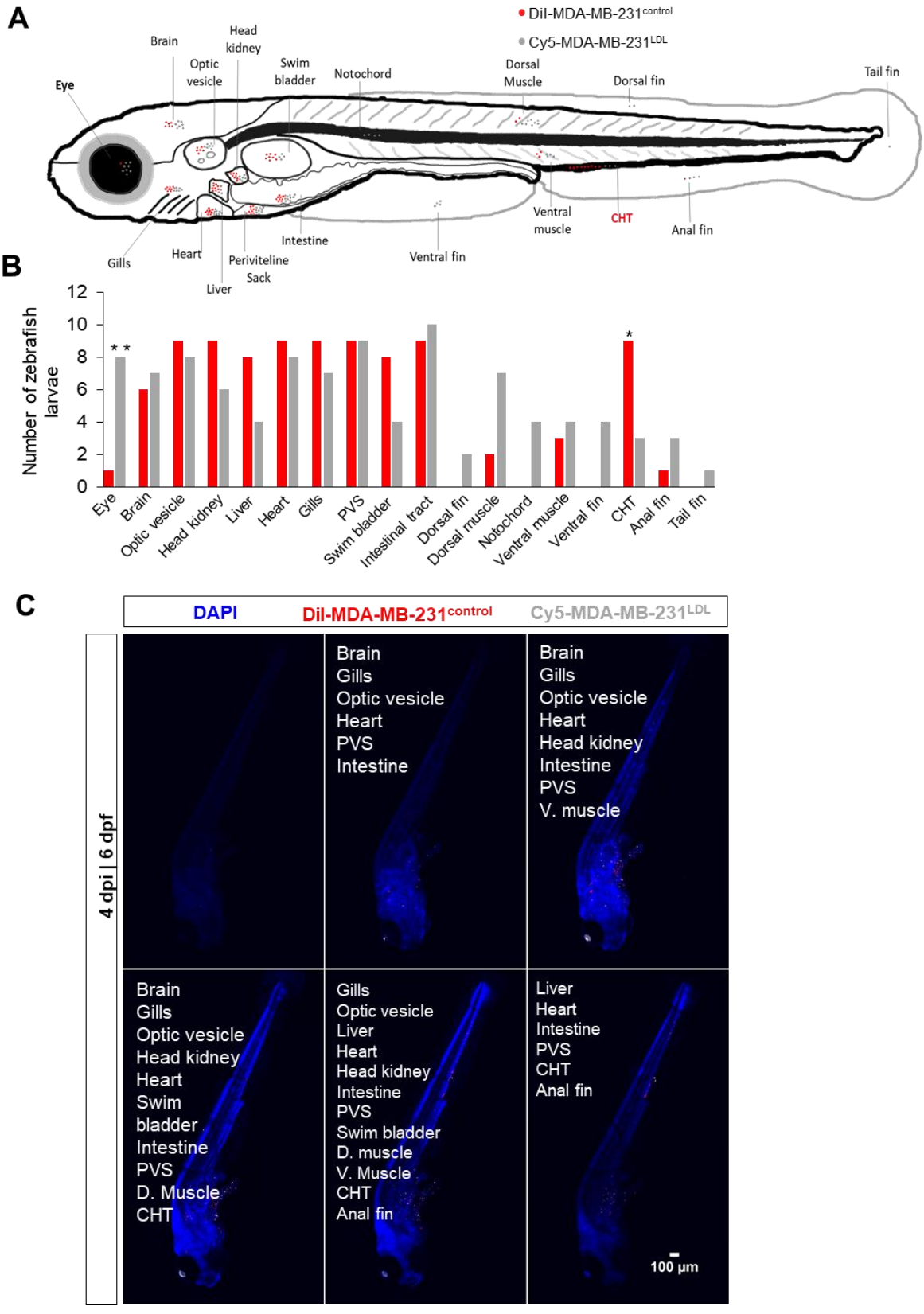

Figure 6: TNBC MDA-MB-231 cells exposed to LDL show differential metastatic tropism to distant sites in xenotransplanted 4dpi zebrafish larvae.

A. Schematic representation of MDA-MB-231 cells invasion potential at 4dpi (6dpf) throughout the zebrafish body with DiI-labelled MDA-MB-231 control (red) and Cy5-labelled LDL-exposed (grey) cells detected in the indicated organs (bold depicts regions with increase tropism, each dot

represents one xenograft. Bold depicts regions with statistical significance for MDA-MB-231LDL(black); MDA-MB-231control (red).

B. Quantification of the invasive potential depicted as the number of zebrafish larvae xenografts (n=11 from 1 independent experiment) with DiI-labelled MDA-MB-231 control (red) and Cy5-labelled LDL-exposed (grey) cells in the indicated organs. Statistic significance was determined by the Fisher test.* $p<0.05$ and ** $p<0.01$.

C. Representative images of whole zebrafish tile (4dpi and 6dpf), with invaded organs, as detailed in each image: brain, gills, optic vesicle, heart, perivitelline space (PVS), intestine, head kidney, ventral muscle, head kidney, swim bladder, dorsal muscle, caudal hematopoietic tissue (CHT), liver, anal fin. Invasion by DiI-labelled MDA-MB-231 control (red) and Cy5-labelled LDL-exposed (grey) cells was captured with spinning disk inverted confocal microscope Zeiss Cell Observer SD. Nuclei staining with DAPI is in blue.

Similarly to the previous analysis obtained with widefield microscopy (Figure 5), confocal imaging (Figure 6 and Supplementary Table 2) also revealed a trend towards differential migration in general (Chi-square p=0.06, n=11) which could potentially reach statistical significance by increasing the number of larvae analysed. Moreover, this analysis also allowed us to detect vessels and previously undetected cells, to identify artefact particles, to better discriminate organ borderlines in all layers and thus to accurately define cell position in relation to the considered organ borderlines. According to our sample, Zeiss Axiovert 200M efficiency to identify invaded organs in zebrafish was 72,03% (206 out of 286 organs were correctly evaluated).

Results obtained show: 1) MDA-MB-231^{LDL} are able to migrate to all organs analysed, contrary to MDA-MB-231^{control}; 2) MDA-MB-231^{control} disseminate according to a gradient, accumulating more in central and vascularised areas and failing to disseminate to distant and less vascularised regions, 3) MDA-MB-231^{LDL} diverged from this pattern, invading also more peripheral, less vascularised organs.

Highly vascularised organs were invaded by cells of both conditions: MDA-MB-231^{LDL} (more in brain and intestinal tract) and MDA-MB-231^{control} (more in gills, heart, head kidney, liver, swim bladder, optic vesicle, and specially CHT (Fisher test, p=0.02), where lies a dense plexus unifying caudal artery and caudal vein[88], (see Supplementary Figure 2) but no other organs reached statistical significance.

Less vascularised organs were invaded preferentially by MDA-MB-231^{LDL}. Amongst these, some were pierced by collateral vessels (dorsal muscle and ventral muscle), by a single vessel (eye, Fisher test, p=0.0075) or lied just beneath CHT (anal fin) and still were invaded by MDA-MB-231^{control}; but others (notochord, ventral fin, dorsal fin, tail fin) have no vessels or at least angiographic studies and our larvae Tg (*fli1:eGFP*) did not show vessels at 6dpf (see Supplementary Figure 2) and were **exclusively infiltrated** by MDA-MB-231^{LDL}.This suggests exposure to LDL accelerated migration through vascular system to peripheral areas.

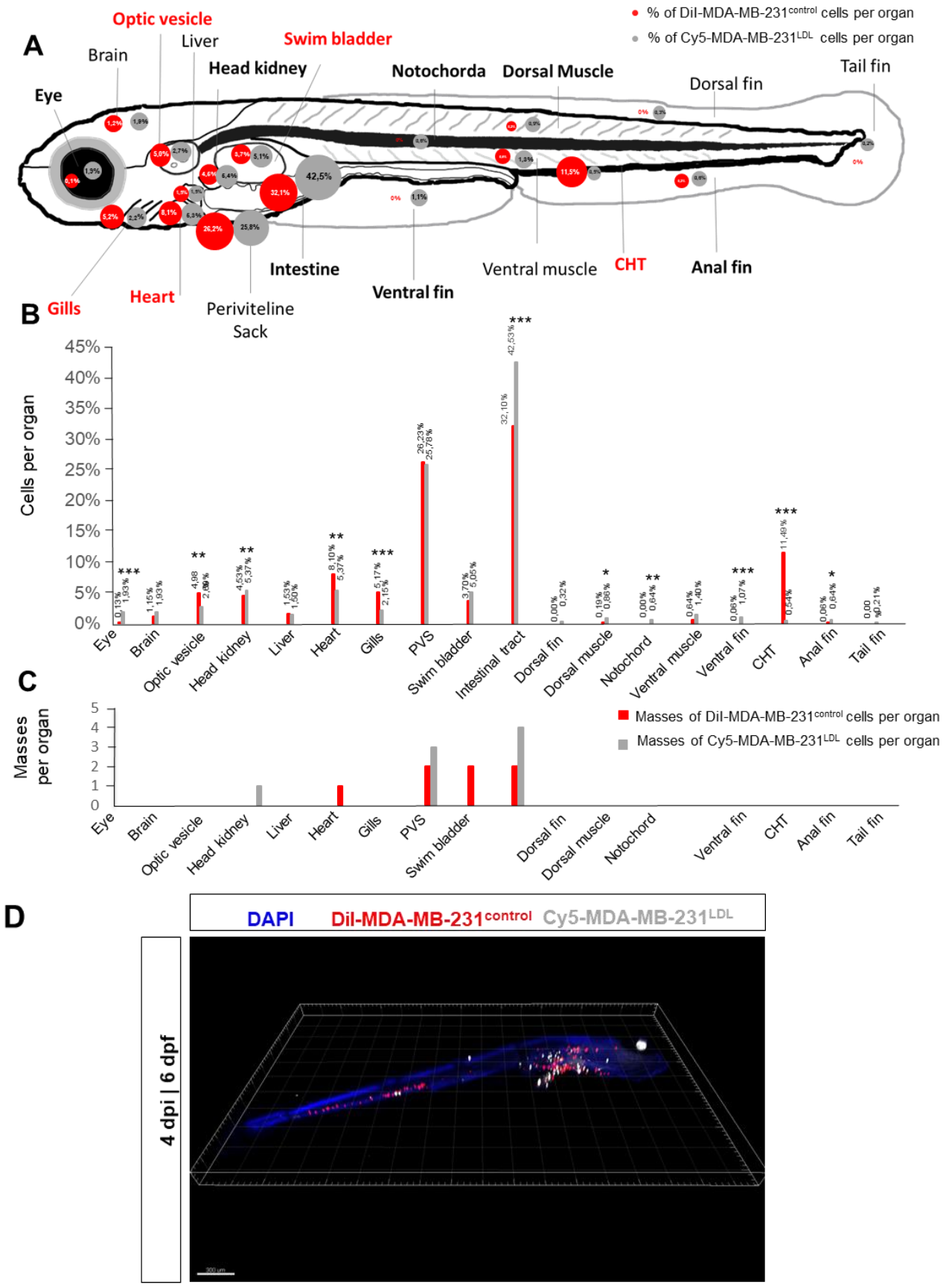

Figure 7: TNBC MDA-MB-231 cells exposed to LDL show differential metastatic tropism to distant sites in xenotransplanted 4dpi zebrafish larvae.

A. Schematic representation of the total distribution of labelled MDA-MB-231 control (red, n=1567 cells) and Cy5-labelled LDL-exposed (grey, n=931 cells) counted throughout the body of 11 zebrafish larvae, each circle represents the proportion of cells of each condition in that organ. Bold depicts regions with statistical significance for MDA-MB-231LDL(grey); MDA-MB-231control (red).

B. Quantification of the distribution depicted as the percentage of DiI-labelled MDA-MB-231 control (red) and Cy5-labelled LDL-exposed (grey) cells thorough the indicated organs. Statistic significance was determined by the Chi-square.* $p<0.05$, ** $p<0.01$, *** $p<0.0001$

C. Quantification of tumour masses (>20 cells) depicted as the number of zebrafish larvae xenografts (n=11 from 1 independent experiment) with DiI-labelled MDA-MB-231 control (red) and Cy5-labelled LDL-exposed (grey) masses in the indicated organs. Statistic significance was determined by the Fisher test.* $p<0.05$ and ** $p<0.01$.

D. Representative 3D reconstruction of the zebrafish tile represented in C (4dpi and 6dpf), invaded by DiI-labelled MDA-MB-231 control (red) and Cy5-labelled LDL-exposed (grey) cells, captured with spinning disk inverted confocal microscope Zeiss Cell Observer SD and processed with Imaris 9.0.1. Nuclei staining with DAPI is in blue.

In order to evaluate the distribution of MDA-MB-231^{LDL} and MDA-MB-231^{control} cells across the zebrafish body, we additionally counted the number of cells in the zebrafish organs (

Figure 7A-C and Supplementary Table 3, n=931 MDA-MB-231^{LDL} and n=1567 MDA-MB-231^{control} cells). Although the total number of cells injected per larvae is roughly known (see Materials and Methods), still we cannot infer if there was a differential survival or proliferation between control and LDL-exposed cells as the exact number of injected cells from each condition could have differ between larvae. Also, tumour masses are highly dense and it is infeasible to count the cells within. However, amongst cells of the same condition, and having in account the number of cells and tumour masses we can infer which organs are preferentially invaded.

MDA-MB-231^{LDL} cells were found in all organs, as previously observed. The difference to MDA-MB-231^{control} was statistically significant in the intestine (Chi-square, $p<0.0001$) and less vascularised organs: eye (Chi-square, $p<0.0001$), dorsal muscle (Chi-square, $p=0.0336$), notochord (Chi-square, $p=0.0058$), ventral fin (Chi-square, $p=0.0002$) and anal fin (Chi-square, $p=0.0236$) and MDA-MB-231^{LDL} cells were observed in areas without vessels.

MDA-MB-231^{control} cells were found in higher proportion in extremely vascularised organs, such as optic vesicle (Chi-square, $p=0.0073$), heart (Chi-square, $p=0.0126$), gills (Chi-square, $p=0.0003$) and CHT (Chi-square, $p<0.0001$) and other regions without reaching statistical significance (PVS, liver). Of these, CHT was the most significant outstanding difference (MDA-MB-231^{control}, n=180 cells; MDA-MB-231^{LDL}, n =5 cells).

Tumour cell masses (>20 cells) were spotted within the organs previously analysed. Results show MDA-MB-231^{LDL} were able to grow 8 tumour cell masses and MDA-MB-231^{control} were able to grow 7 (Figure 6A and B). Of these, distant tumour cell masses accounted 5 for both MDA-MB-231^{LDL} and MDA-MB-231^{control}. There was no difference in the number of distant masses or relevant difference in number of overall masses. However, MDA-MB-231^{LDL} masses were predominantly grown in intestine and PVS, and one in head kidney, while MDA-MB-231^{control} cells grew less masses in intestine and PVS but were able to grow two masses in the highly vascularised swim bladder and one in the heart.

Also, it must be pointed out that, although swim bladder has more MDA-MB-231^{LDL} cells, MDA-MB-231^{control} cells were able to grow two tumour masses within it. As tumour masses are extremely dense it was not possible to include these structures in the quantification of cells count cells, but having in account these masses, swim bladder was more invaded by MDA-MB-231^{control} cells. All other masses were present in the condition (control or LDL) that also present increase number of (countable) cells in that organ, such as the PVS, intestine, heart, head kidney.

3.3 Impact of LDL exposure in the mitochondrial network distribution of TNBC cells xenotransplanted into zebrafish larvae: qualitative assessment

Since alterations in mitochondrial mass, biogenesis and dynamics have been implicated in the acquisition of more aggressive and migratory behaviour of cancer cells,[58,60] next, we went on to determine the impact of LDL exposure in the mitochondrial network distribution of TNBC cells in the larvae using the Mito-YFP signal as a marker for mitochondria.

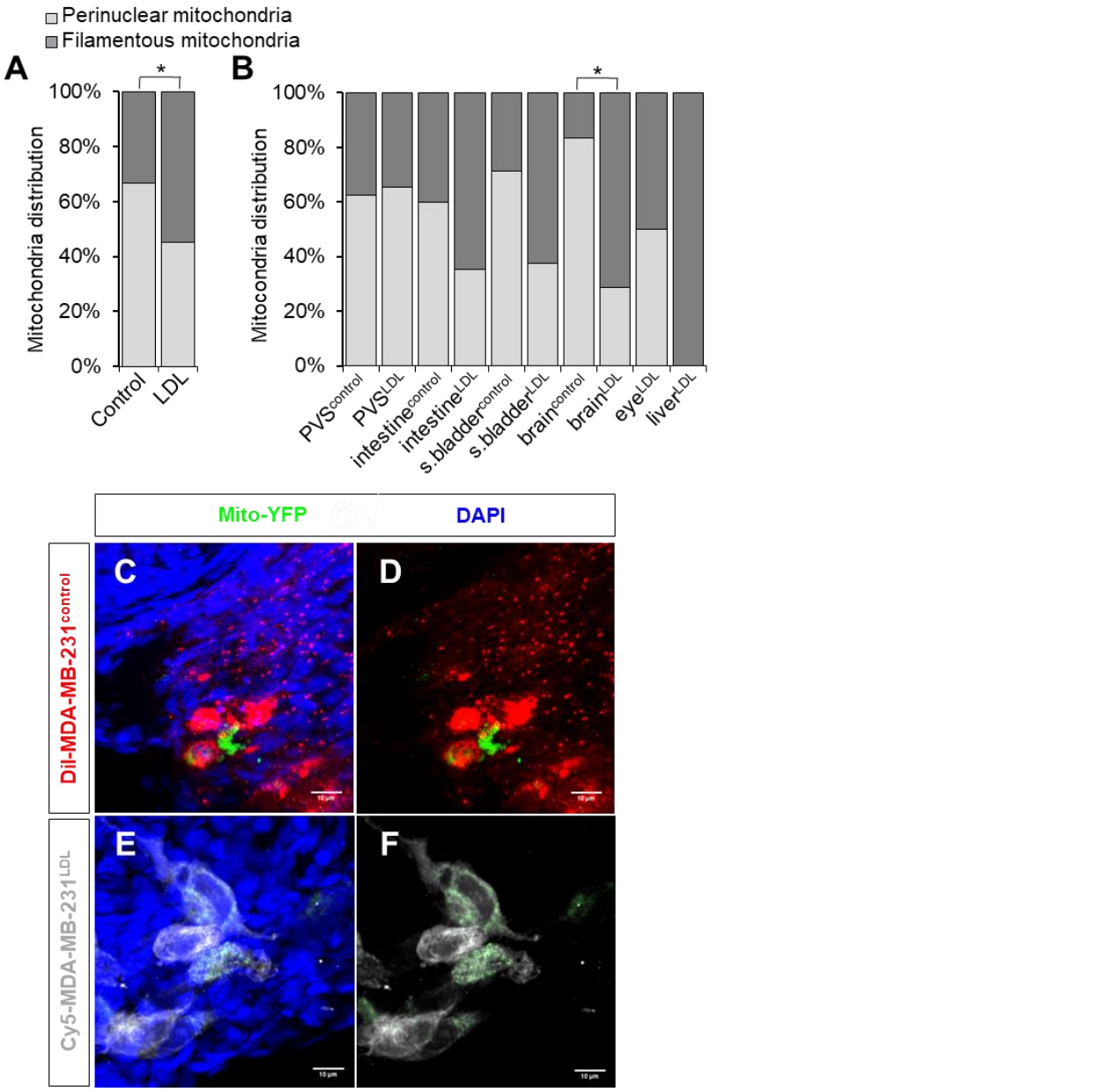

Figure 8: TNBC MDA-MB-231 cells control or exposed to LDL previously transfected with the mitochondrial reporter Mito-YFP were xenotransplanted into 2dpf zebrafish. Cells show a differential mitochondrial network distribution at 4dpi (6dpf).

A. Chart representing the mitochondrial network distribution of MDA-MB-231control (n=39) and MDA-MB-231LDL (n=64) cells in the overall quantified organs from xenotransplated zebrafish larvae at at 4dpi.

B. Chart representing the mitochondrial network distribution of MDA-MB-231control (n=16 PVS, n=10 intestine, n=7 swim bladder, n=6 brain) and MDA-MB-231LDL (n=29 PVS, n=17 intestine, n=8 swim bladder, n=5 brain, n=2 eye, n=3 liver) cells in each organ from xenotransplated zebrafish larvae at at 4dpi. Statistic significance was determined by the Fisher test.* $p<0.05$

C – F. Representative images of maximum intensity projection of a DiI-labelled MDA-MB-231control (red) cell with perinuclear mitochondrial network distribution labelled with Mito-YFP (green). Nuclei are labelled with DAPI (blue) acquired from the PVS zebrafish xenotransplanted larvae at 4dpi with point scanning fluorescence microscope Zeiss LSM 880 (C, D). Representative images of maximum intensity projection of a Cy5-labelled MDA-MB-231LDL (grey) cell with perinuclear mitochondrial network labelled with Mito-YFP (green) and DAPI (nuclei, blue)

acquired from the eye of zebrafish xenotransplanted larvae at 4dpi with point scanning fluorescence microscope Zeiss LSM 880 (E, F).

Our results (
Figure 8) show that, in general, 54.7% of MDA-MB-231^{LDL} cells have a filamentous distribution of mitochondrial network compared to 33.3% of MDA-MB-231^{control} (Fisher Test, p=0.0429).

Filamentous distribution represents the following share of MDA-MB-231^{LDL} and MDA-MB-231^{control} cells analysed: in PVS (34.5% and 37.5%, respectively), in intestine (64.7% and 40%, respectively), in swim bladder (62.5% and 28.6%, respectively), in brain (100% and 16.7%, respectively), eye (50% and no Mito-YFP positive cells were found for MDA-MB-231^{control}) and liver (100% and no Mito-YFP positive cells were found for MDA-MB-231^{control}). LDL seems to have favoured a more filamentous mitochondrial distribution, associated with increased invasion of intestine and brain (p=0.0152). Eye and liver did not have comparison since we did not found MDA-MB-231^{control} cells with marked expression of Mito-YFP to be compared.

3.4 Impact of LDL exposure in the mitochondrial network distribution of TNBC cells xenotransplanted into zebrafish larvae: quantitative assessment

Our aim was to determine whether exposure to LDL would lead to the changes in the mitochondrial network of migrating cells and if those would be correlated to higher aggressiveness. We performed a quantitative analysis of the confocal acquisitions of mitochondrial network, using FIJI software.[89] The sub z-stack of each cell was acquired and converted into maximum intensity projections; Mito-YFP channel and membrane channel (DiI or Cy5) were processed into binary images (Supplementary Figure 3) and the area and number of Mito-YFP and DiI/Cy5 particles was determined.

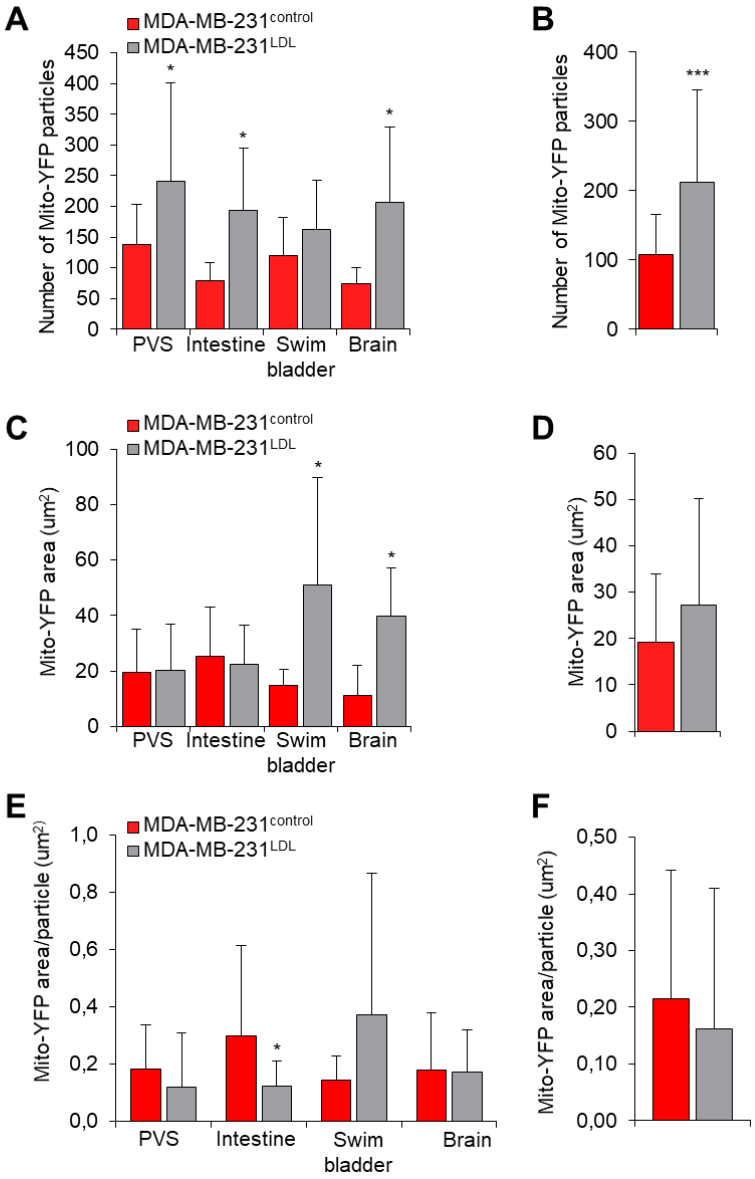

Figure 9: Quantification of mitochondria network distribution in Mito-YFP transfected MDA-MB-231 control and LDL-exposed cells xenotransplanted into zebrafish larvae at 2dpf and analysed at 4dpi (6dpf)).

A - B. Charts representing the number of Mito-YFP-labelled mitochondria particles per MDA-MB-231control (n=13 PVS, n=10 intestine, n=7 swim bladder, n=5 brain) and MDA-MB-231LDL (n=26 PVS, n=16 intestine, n=8 swim bladder, n=5 brain) cell (A) and the average number of Mito-YFP-labelled mitochondria particles in total (n=35 MDA-MB-231control and n=55 MDA-MB-231 LDL cells) (B).

C-D. Charts representing the area of Mito-YFP-labelled mitochondria per MDA-MB-231control (n=13 PVS, n=10 intestine, n=7 swim bladder, n=5 brain) and MDA-MB-231LDL (n=26 PVS, n=16 intestine, n=8 swim bladder, n=5 brain) cell (C) and the average number of Mito-YFP-labelled mitochondria particles in the total (n=35 MDA-MB-231control and n=55 MDA-MB-231 LDL cells) (D).

E-F. Charts representing the area of Mito-YFP-labelled mitochondria per particle in MDA-MB-231control (n=13 PVS, n=10 intestine, n=7 swim bladder, n= 5 brain) and MDA-MB-231LDL (n=26 PVS, n=16 intestine, n=8 swim bladder, n=5 brain) cells (E) the average area of YFP-labelled mitochondria per particle in total (n=35 MDA-MB-231control and n=55 MDA-MB-231 LDL cells) (F).

Statistic significance was determined by the Student T-test (unpaired, two-tailed). * $p<0.05$, ** $p<0.01$, *** $p<0.0001$.

Results (Figure 9) show an overall increased number of Mito-YFP particles in MDA-MB-231 cells previously exposed to LDL: MDA-MB-231^{LDL} average 212.6 Mito-YFP particles per cell (n=55), while MDA-MB-231^{control} average 108.2 Mito-YFP particles per cell (n=35; Student T-student, $p<0.0001$). Also, this difference was statistically significant in most of the organs analysed, including PVS ($p=0.0304$), intestine ($p=0.0022$) and brain (T-student, $p=0.0456$). This suggests LDL increases the number of mitochondria in MDA-MB-231 cells.

Also, we quantified the average area of Mito-YFP particles in MDA-MB-231 cells and in total, MDA-MB-231^{LDL} cells averaged 27.2 μm^2 (n=55) whereas MDA-MB-231^{control} cells averaged 19.2 μm^2 (n=35), which was not statistically significant (Student T-test, $p=0.0723$). Though, this difference was statistically significant in the Swim bladder (Student T-test, $p=0.0283$) and the brain (T-student, $p=0.0237$). Increased Mito-YFP area in MDA-MB-231 cells seems to be promoted by LDL.

Finally, we determined the average area of Mito-YFP particles in MDA-MB-231 cells as this reflects the size of mitochondria. In total, MDA-MB-231^{LDL} cells had inferior average area (0.191 μm^2/particle, n=55) than MDA-MB-231^{control} cells (0.239 μm^2/particle, n=34)) although this was not statistically significant (Student T-student, $p=0.383$). The difference was statistically significant in the intestine (Student T-student, $p=0.0084$). This suggests LDL may reduce Mito-YFP area per particle in MDA-MB-231 cells, despite failing to induce this phenotype in the swim bladder.

4 DISCUSSION

Our tropism results suggest that MDA-MB-231^{LDL} cells have greater ability to invade since all organs were invaded by these cells, on both studies. This divergence stands out in less vascularised and distant to inoculation sites (dorsal fin, dorsal muscle, notochord, anal fin - as seen in Figure 5; dorsal fin, dorsal muscle, ventral fin, notochord, anal fin, eye - as seen in Figure 6). The metastatic cascade involves local invasion into surrounding tissues; intravasation to circulatory system; survival during hematogenous transit; arrest; extravasion; formation of micrometastatic colonies and further colonization.[18] In this experiment, cells of both conditions were able to undertake the first 3 steps, invading, intravasating vessels and surviving hematogenous dissemination, as observed in highly vascularised CHT. However, peripheral organs where no vessels where seen[88] (Supplementary Figure 2), were significantly more infiltrated by MDA-MB-231^{LDL} cells. Since LDL apparently increased MDA-MB-231 cells dissemination we wondered why this phenomenon occurred, ie., why did MDA-MB-231^{LDL} display faster/or more invasive/independent from vascularization migratory properties when compared to MDA-MB-231^{control} cells.

Counting the number of cells in each organ gave us an overview at the full frame of migration in the whole organism and differential cell distribution. It stood out the significant accumulation of MDA-MB-231^{control} cells (n=180) in CHT and the absence in close areas such as tail fin, notochord or any area without detectable vessels at 6 dpf (except anal fin, in which MDA-MB-231^{control} n=1). In other organs this phenotype was also observed including highly vascularised organs of the trunk (intestine and swim bladder) and no MDA-MB-231^{control} cells were found close to these organs, nor in ventral fin neither in notochord. Two hypotheses might explain this result: 1) chemoattraction of MDA-MB-231^{control} cells specifically to vascularised areas; 2) increased aggressiveness of MDA-MB-231^{LDL} cells endowed with increased ability to extravasate or survive outside hematogenous transit or both, compared to MDA-MB-231^{control} which accumulated inside vessels, particularly in CHT (n=180, median=16, Figure 3, Supplementary Table 3) in which extravasation and/or survival in nearby organs seemed to be limiting. Thus, as cells share the same microenvironment this frame suggests the extravasation and survival at distance might be promoted upon LDL exposure through transformations in the cancer cells. Literature describes invadopodium as cytoplasmic protrusions of transformed cells that play a role on extravasating, breaching the endothelial junctions.[50] These seem to require cholesterol to form;[38,93] hence LDL might endow MDA-MB-231 cells with increase ability to form invadopodia and extravasate. In general, anchoring and surviving at distance is sustained by the ability of TNBC cells to switch to FAO[65] In our experiments, exposition of TNBC cells to LDL-containing medium might have provided a supply of lipids, as demonstrated by increased Bodypy

detection of lipid droplets inside in MDA-MB-231^{LDL} cells (Supplementary Figure 1). It is possible that FAO may also be enhanced as expression of CD36 is upregulated upon exposure to dietary lipids,[65] and increase FAO and ETC-related-ATP synthesis in general are upregulated by genes and proteins in MDA-MB-231[71] but further studies would be necessary to confirm increased FAO at distance in MDA-MB-231^{LDL} cells.

Tumour masses evaluation did not reveal significant differences. Future studies with evaluation of xenotransplanted larvae at later time points and with MDA-MB-231^{LDL} and MDA-MB-231^{control} cells injected in separate larvae will be needed to correctly evaluate the ability of TNBC cells to colonize and grow masses at distance since this is a latter phenomenon in the metastatic cascade and thus hardly happened in this 4 dpi model. Moreover, co-injection of cells might not be the best model since secretion of exosomes and/or metabolites by MDA-MB-231^{LDL} cells might modulate local or distant microenvironment, paving the way for its counterpart MDA-MB-231^{control} cells to metastize or vice-versa.[75]

Our evaluation of mitochondrial network distribution revealed that MDA-MB-231^{LDL} cells assumed a more filamentous distribution, i.e. mitochondria were across the entirety of the cell, diverging from MDA-MB-231^{control} cells that majorly present perinuclear mitochondrial network distribution. As we considered that MDA-MB-231^{LDL} cells had increase metastatic potential (explained before), the adoption of a more distributed mitochondrial network could be favouring metastatic progression. Particularly at distance (intestine, swim bladder, brain, eye, liver), MDA-MB-231^{LDL} cells seem to acquire a more filamentous mitochondrial network (only consistent for the brain for all the quantifications performed). It is possible that acquisition of a more widespread and filamentous mitochondria distribution across the cell has implications in the migratory and invasive behaviour of TNBC cells since most of the MDA-MB-231^{LDL} cells that achieved migration to distant sites displayed an increased proportion of filamentous mitochondrial distribution compared to MDA-MB-231^{LDL} cells located in the PVS (although also presenting increase number of particles) or its counterparts MDA-MB-231^{control} cells. Results are in conformity with Senf and Ronai, et al. and others which proposed that in migrating cancer cells, mitochondria are transported to the leading edges of the cell[58] and were carried to cytoplasmatic protrusions where they played a role on its assembly and function, increasing migration and invasion.[37,94]

Also, literature described that mitochondria of migrating cells undergo fission, so that it can be transported along the cytoskleton.[94,95]

We quantified mitochondrial network total number of Mito-YFP particles, area of Mito-YFP per cell and area of Mito-YFP per particle in MDA-MB-231^{control} and MDA-MB-231^{LDL} cells. Mitochondria were transfected with Mito-YFP (see Materials and Methods), therefore in maximum intensity projections Mito-YFP number of particles is an indirect measure of mitochondrial mass; whereas Mito-YFP area is an indirect measure of mitochondrial area distribution across the cell and Mito-YFP area per particle is an indirect measure of mass/size of each mitochondrion. Our results suggest that LDL increased average mitochondrial mass but lowered mass per mitochondrion and favoured increased area of distribution of mitochondria. In other words, MDA-MB-231^{LDL} cells seem to have upregulated mitochondrial biogenesis, which LeBleu[60] suggested was a feature of BC initiating its path to invade and migrate, to have undergone increased fission and widespread distribution, which Senft and Ronai, et.al[58] proposed to be essential for cancer cell invasion and migration. In the one organ (swim bladder) LDL exposure may not have been enough to induce fission (MDA-MB-231^{LDL} had increased Mito-YFP area per particle), other stimuli might have played a role. Interestingly, in this organ, the number of MDA-MB-231^{LDL} and MDA-MB-231^{control} cells was very similar but MDA-MB-231^{control} have grown 2 tumour masses, indicating that in this organ, LDL failed to promote increased invasion, survival and proliferation.

Altogether, LDL seems to have induced a general increase in migratory and invasive properties in MDA-MB-231^{LDL} cells in in xenotransplanted zebrafish larvae. Potentially several mechanisms could explain this phenotype, but transformations in cancer cells seem to underlie these phenotypes since local and distant microenvironment was common. Such transformations may have endowed MDA-MB-231^{LDL} cells with increased extravasation and survival at distance potential, but further research should confirm these results.

Also, mitochondrial adaptations detected in LDL-exposed cells seem to correlate to the increased ability of TNBC cells to migrate/invade diastal organs in xenotransplanted zebrafish larvae. Such adaptations include increase proportion of cells displaying mitochondrial filamentous network distribution; increased number and area occupied by the Mito-YFP particles but decreased mitochondria size (Mito-YFP area per particle). These mitochondrial transformations may be one of the mechanisms whereby LDL increases invasion, migration and/or survival at distance.

There were some limitations in our experiment. Firstly, MDA-MB-231^{LDL} and MDA-MB-231^{control} were coinjected into each zebrafish larvae, raising the question of whether MDA-MB-231^{control} invasive behaviour could be moulded by MDA-MB-231^{LDL} cells interference through release of

exossomes to the microenvironment or matrix remodelling, for instance. Also, concern with zebrafish tumour microenvironment must be raised. Although 2-6dpf zebrafish replicates interactions with innate system,[96] vascular cells[83] and different organs,[83] the influence of the microenvironment goes beyond that, and zebrafish may not simulate the human local and distant microenvironment as cancer cells take up fatty acids, glucose, amino acids that mould its metabolism and many factors may influence cancer cells epigenetics.[83]

Our results raise further concerns that should be tested with improved experimental design. The injection of MDA-MB-231^{LDL} and MDA-MB-231^{control} cells in separate larvae labelled with the same lipophilic dye (preferentially Cy5) must confirm these results and exclude interferences of co-injection procedure. Live-imaging at two distinct time-points (1 e 4 dpf) and termination of the experiments at 6dpf will allow following the path of cells since injection until the development of more considerable masses as well as studying LDL role on cell survival. Using Tg (*fli1:eGFP*) only and an alternative mitochondrial marker emitting outside the green spectrum would facilitate detection of MDA-MB-231 cells in which Mito-YFP marker was effective while enabling further analysis of cancer cell-endothelial interaction. Determining whether cells at distance undergo fatty acid oxidation and the relation between mitochondria and cell protrusions would clarify part of the lipid metabolism role on TNBC cells. Regarding the bioimaging acquisition, confocal microscopy (63x oil) to address the mitochondrial network, confocal microscopy tiles with 20x amplification for tropism study and measuring mitochondrial volume (instead of mitochondrial indirect measures in maximum intensity projections) using Imaris 9.0.1.

Future hope to treat metastatic TNBC through new therapeutic targets may point at inhibiting FAO but further studies are needed to clarify FAO role on metastasis and to identify safe targets. Particularly in MYC[68] and AKR1B10[69] overexpressing TNBC, therapeutic efficiency might be elevated since these subsets of TNBC are highly dependent upon FAO.[68,69] MYC[68] and AKR1B10[69] are defining factors that upregulate FAO and downregulate fatty acid synthesis and thus might be predictor markers for successful FAO inhibitory therapeutic[68,69] that might be directed at CD36,[65] CDCP1,[71] or at inhibiting other components of altered lipid metabolism.[71] Acting at complementary points of metastatic cascade may be useful, aiming at eradicating established metastasis, preventing growth and colonization at distance and avoiding dissemination of tumour.[19]

5 REFERENCES

1. Savci-Heijink C, Halfwerk H, Hooijer G, Horlings H, Wesseling J, Vijver M. Retrospective analysis of metastatic behaviour of breast cancer subtypes. *Breast Cancer Res Treat*. 2015;150:547-557. doi:10.1007/s10549-015-3352-0

2. Cummings MC, Simpson PT, Reid LE, et al. Metastatic progression of breast cancer: Insights from 50 years of autopsies. *J Pathol*. 2014;232(1):23-31. doi:10.1002/path.4288

3. Bray F, Ferlay J, Soerjomataram I, Siegel RL, Torre LA, Jemal A. Global Cancer Statistics 2018: GLOBOCAN Estimates of Incidence and Mortality Worldwide for 36 Cancers in 185 Countries. *CA Cancer J Clin*. 2018:1-31. doi:10.3322/caac.21492

4. Giuliano AE, Connolly JL, Edge SB, et al. Breast Cancer-Major changes in the American Joint Committee on Cancer eighth edition cancer staging manual. *CA Cancer J Clin*. 2017;67(4):290-303. doi:10.3322/caac.21393

5. Kimbung S, Loman N, Hedenfalk I. Clinical and molecular complexity of breast cancer metastases. *Semin Cancer Biol*. 2015;35:85-95. doi:10.1016/j.semcancer.2015.08.009

6. Gobbini E, Ezzalfani M, Dieras V, et al. Time trends of overall survival among metastatic breast cancer patients in the real-life ESME cohort. *Eur J Cancer*. 2018;96:17-24. doi:10.1016/j.ejca.2018.03.015

7. Caswell-jin JL, Plevritis SK, Tian L, et al. Change in Survival in Metastatic Breast Cancer with Treatment Advances : Meta-Analysis and Systematic Review. *JNCI Cancer Spectr*. 2018;2(4):1-10. doi:10.1093/jncics/pky062

8. Perou CM, Sùrlie T, Eisen MB, et al. Molecular portraits of human breast tumours. *Nature*. 2000;406:747-752.

9. Sørlie T, Perou CM, Tibshirani R, et al. Gene expression patterns of breast carcinomas distinguish tumor subclasses with clinical implications. *PNAS*. 2001;98(19):10869–10874.

10. Harbeck N, Gnant M. Breast cancer. *Lancet*. 2017;389:1134-1150. doi:10.1016/S0140-6736(16)31891-8

11. Foulkes WD, Ian E. Smith, Reis-Filho JS. Triple-Negative Breast Cancer. *N Engl J Med*. 2010;363:1938-1948.

12. Bianchini G, Balko JM, Mayer IA, Sanders ME, Luca Gianni. Triple-negative breast cancer: challenges and opportunities of a heterogeneous disease. *Nat Rev Clin Oncol*. 2016;13(11):674-690. doi:10.1038/nrclinonc.2016.66

13. Jitariu A, Cîmpean AM, Ribatti D, Raica M. Triple negative breast cancer: the kiss of death. *Oncotarget*. 2017;8(28):46652-46662.

14. Hanahan D, Weinberg RA. Hallmarks of Cancer: The Next Generation. *Cell Rev*.

2011;144(5):646-674. doi:10.1016/j.cell.2011.02.013

15. Fidler IJ. The pathogenesis of cancer metastasis: the "seed and soil" hypothesis revisited. *Nat Rev Cancer*. 2003;3(June):1-6.

16. Gupta GP, Massagué J. Cancer Metastasis: Building a Framework. *Cell*. 2006;127:679-695. doi:10.1016/j.cell.2006.11.001

17. Valastyan S, Weinberg RA. Tumor metastasis: Molecular insights and evolving paradigms. *Cell*. 2011;147(2):275-292. doi:10.1016/j.cell.2011.09.024

18. Lambert AW, Pattabiraman DR, Weinberg RA. Emerging Biological Principles of Metastasis. *Cell*. 2017;168(4):670-691. doi:10.1016/j.cell.2016.11.037

19. Lorusso G, Rüegg C. New insights into the mechanisms of organ-specific breast cancer metastasis. *Semin Cancer Biol*. 2012;22(3):226-233. doi:10.1016/j.semcancer.2012.03.007

20. Danaei G, Finucane MM, Lu Y, et al. National, regional, and global trends in fasting plasma glucose and diabetes prevalence since 1980: systematic analysis of health examination surveys and epidemiological studies with 370 country-years and 2,7 million participants. *Lancet*. 2011;378:31-40. doi:10.1016/S0140-6736(11)60679-X

21. Afshin A, Forouzanfar MH, Reitsma MB, et al. Health Effects of Overweight and Obesity in 195 Countries over 25 Years. *N Engl J Med*. 2017;377(1):13-27. doi:10.1056/NEJMoa1614362

22. Boyle P, Boniol M, Koechlin A, et al. Diabetes and breast cancer risk: a meta-analysis. *Br J Cancer*. 2012;107(9):1608-1617. doi:10.1038/bjc.2012.414

23. Barone BB, Hsin-Chieh Y, Snyder CF, et al. Long-term All-Cause Mortality in Cancer Patients With Preexisting Diabetes Mellitus. *JAMA*. 2008;300(23):2754-2764.

24. Jiralerspong S, Goodwin PJ. Obesity and Breast Cancer Prognosis: Evidence, Challenges, and Opportunities. *J Clin Oncol*. 2016;34(35):4203-4216. doi:10.1200/JCO.2016.68.4480

25. Garcia-Estevez L, Moreno-Bueno G. Updating the role of obesity and cholesterol in breast cancer. *Breast Cancer Res*. 2019;21(35):1-8. doi:10.1186/s13058-019-1124-1

26. Eckel RH, Grundy SM, Zimmet PZ. The metabolic syndrome. *Lancet*. 2005;365:1415-1428.

27. Buono G, Crispo A, Giuliano M, et al. Combined effect of obesity and diabetes on early breast cancer outcome: a prospective observational study. *Oncotarget*. 2017;8(70):115709-115717.

28. Mcdonnell DP, Park S, Goulet MT, et al. Obesity, Cholesterol Metabolism, and Breast Cancer Pathogenesis. *Cancer Res*. 2014;74(18):4976-4983. doi:10.1158/0008-5472.CAN-14-1756

29. Baek AE, Nelson ER. The Contribution of Cholesterol and Its Metabolites to the Pathophysiology of Breast Cancer. *Horm Cancer*. 2016;7(4):219-228. doi:10.1007/s12672-

016-0262-5

30. Hevonoj T, Pentikainen M, Hyvonen M, Kovanen P, Ala-Korpela M. Structure of low density lipoprotein (LDL) particles: Basis for understanding molecular changes in modi¢ed LDL. *Biochim Biophys Acta*. 2000;1488:189-210. doi:10.1299/kikaia.71.346

31. Santos R D, Catarina, Domingues G, et al. LDL-cholesterol signaling induces breast cancer proliferation and invasion. *Lipids Health Dis*. 2014;13(1):16.

32. Simons K, Ikonen E. Functional rafts in cell membranes. *Nature*. 1997;387:569-572.

33. Rodrigues dos Santos C, Fonseca I, Dias S, de Almeida JCM. Plasma level of LDL-cholesterol at diagnosis is a predictor factor of breast tumor progression. *BMC Cancer*. 2014;14(1):1-10. doi:10.1186/1471-2407-14-132

34. Bahl M, Ennis M, Tannock IF, et al. Serum lipids and outcome of early-stage breast cancer: results of a prospective cohort study. *Breast Cancer Res Treat*. 2005;94:135-144. doi:10.1007/s10549-005-6654-9

35. Llaverias G, Danilo C, Mercier I, et al. Role of Cholesterol in the Development and Progression of Breast Cancer. *Am J Pathol*. 2011;178(1):402-412. doi:10.1016/j.ajpath.2010.11.005

36. Eckert MA, Yang J. Targeting invadopodia to block breast cancer metastasis. *Oncotarget*. 2011;2(7):562-568.

37. Zhao J, Zhang J, Yu M, et al. Mitochondrial dynamics regulates migration and invasion of breast cancer cells. *Oncogene*. 2013;32:4814-4824. doi:10.1038/onc.2012.494

38. Yamaguchi H, Takeo Y, Yoshida S, Kouchi Z, Nakamura Y, Fukami K. Lipid rafts and caveolin-1 are required for invadopodia formation and extracellular matrix degradation by human breast cancer cells. *Cancer Res*. 2009;69(22):8594-8602. doi:10.1158/0008-5472.CAN-09-2305

39. Caldieri G, Buccione R. Aiming for invadopodia: organizing polarized delivery at sites of invasion. *Trends Cell Biol*. 2009;20(20):64-70. doi:10.1016/j.tcb.2009.10.006

40. Freeman M, Vizio D Di, Solomon KR. The Rafts of the Medusa: cholesterol targeting in cancer therapy. *Oncogene*. 2010;29:3745-3747. doi:10.1038/onc.2010.132

41. Siddiqui RA. Migration of MDA-MB-231 breast cancer cells depends on the availability of exogenous lipids and cholesterol esterification. *Clin Exp Metastasis*. 2011;28:733-741. doi:10.1007/s10585-011-9405-9

42. Bravo-cordero JJ, Hodgson L, Condeelis J. Directed cell invasion and migration during metastasis. *Curr Opin Cell Biol*. 2012;24(2):277-283. doi:10.1016/j.ceb.2011.12.004

43. Magalhaes A, Matias I, Palmela I, Brito MA, Dias S. LDL-cholesterol increases the

transcytosis of molecules through endothelial monolayers. *PLoS One*. 2016;11(10):1-11. doi:10.1371/journal.pone.0163988

44. Reymond N, Borda B, Ridley AJ. Crossing the endothelial barrier during metastasis. *Nat Rev*. 2013;13(12):858-870. doi:10.1038/nrc3628

45. Pelton K, Coticchia CM, Curatolo AS, et al. Hypercholesterolemia Induces Angiogenesis and Accelerates Growth of Breast Tumors in Vivo. *Am J Pathol*. 2014;184(7):2099-2110. doi:10.1016/j.ajpath.2014.03.006

46. Wyckoff JB, Wang Y, Lin EY, et al. Direct Visualization of Macrophage-Assisted Tumor Cell Intravasation in Mammary Tumors. *Cancer Res*. 2007;67(6):2649-2657. doi:10.1158/0008-5472.CAN-06-1823

47. Li YC, Park MJ, Ye SK, Kim CW, Kim YN. Elevated levels of cholesterol-rich lipid rafts in cancer cells are correlated with apoptosis sensitivity induced by cholesterol-depleting agents. *Am J Pathol*. 2006;168(4):1107-1118. doi:10.2353/ajpath.2006.050959

48. Alikhani N, Ferguson RD, Novosyadlyy R, et al. Mammary tumor growth and pulmonary metastasis are enhanced in a hyperlipidemic mouse model. *Oncogene*. 2013;32(8):961-967. doi:10.1038/onc.2012.113

49. Castaneda CA, Cortes-Funes H, Gomez HL, Ciruelos EM. The phosphatidyl inositol 3-kinase/AKT signaling pathway in breast cancer. *Cancer Metastasis Rev*. 2010;29:751-759. doi:10.1007/s10555-010-9261-0

50. Leong HS, Robertson AE, Stoletov K, et al. Invadopodia Are Required for Cancer Cell Extravasation and Are a Therapeutic Target for Metastasis. *Cell Rep*. 2014;8(5):1558-1570. doi:10.1016/j.celrep.2014.07.050

51. Caldieri G, Giacchetti G, Beznoussenko G, Attanasio F, Ayala I, Buccione R. Invadopodia biogenesis is regulated by caveolin-mediated modulation of membrane cholesterol levels. *J Cell Mol Med*. 2009;13(8):1728-1740. doi:10.1111/j.1582-4934.2008.00568.x

52. Nieto MA, Huang RY, Jackson RA, Thiery JP. EMT: 2016. *Cell*. 2016;166:21-45. doi:10.1016/j.cell.2016.06.028

53. Imani S, Hosseinifard H, Cheng J, Wei C, Fu J. Prognostic Value of EMT-inducing Transcription Factors (EMT-TFs) in Metastatic Breast Cancer: A Systematic Review and Meta-analysis. *Sci Rep*. 2016;6(January):1-10. doi:10.1038/srep28587

54. Lu C, Lo Y-H, Chen C-H, et al. VLDL and LDL, but not HDL, promote breast cancer cell proliferation, metastasis and angiogenesis. *Cancer Lett*. 2016;388(December):1-9. doi:10.1016/j.canlet.2016.11.033

55. Nelson ER, Chang C yi, McDonnell DP. Cholesterol and breast cancer pathophysiology. *Trends Endocrinol Metab*. 2014;25(12):649-655. doi:10.1016/j.tem.2014.10.001

56. Ribas V, García-Ruiz C, Fernández-Checa JC. Mitochondria, cholesterol and cancer cell metabolism. *Clin Transl Med*. 2016;5(1):1-24. doi:10.1186/s40169-016-0106-5

57. Mishra P, Chan DC. Mitochondrial dynamics and inheritance during cell division, development and disease. *Nat Rev*. 2014;15(10):634-646. doi:10.1038/nrm3877

58. Senft D, Ronai ZA. Regulators of mitochondrial dynamics in cancer. *Curr Opin Cell Biol*. 2016;39(April 2016):43-52. doi:10.1016/j.ceb.2016.02.001

59. White C. The Regulation of Tumor Cell Invasion and Metastasis by Endoplasmic Reticulum-to-Mitochondrial Ca 2 + Transfer. *Front Oncol*. 2017;7(August):1-8. doi:10.3389/fonc.2017.00171

60. Lebleu VS, Connell JTO, Herrera KNG, et al. PGC-1α mediates mitochondrial biogenesis and oxidative phosphorylation in cancer cells to promote metastasis. *Nat Cell Biol*. 2014;16(10):992-1003. doi:10.1038/ncb3039

61. DeBerardinis RJ, Lum JJ, Hatzivassiliou G, Thompson CB. The Biology of Cancer: Metabolic Reprogramming Fuels Cell Growth and Proliferation. *Cell Metab Rev*. 2008;7:11-20. doi:10.1016/j.cmet.2007.10.002

62. Monaco ME. Fatty acid metabolism in breast cancer subtypes. *Oncotarget*. 2017;8(17):29487-29500. doi:10.18632/oncotarget.15494

63. Carracedo A, Cantley LC, Paolo Pandolfi P. Cancer metabolism: fatty acid oxidation in the timelight. *Nat Rev Cancer*. 2013;13(4):227-232. doi:10.1038/nrc3483

64. Burstein MD, Tsimelzon A, Poage GM, et al. Comprehensive Genomic Analysis Identifies Novel Subtypes and Targets of Triple-Negative Breast Cancer. *Clin Cancer Res*. 2015;21(7):1688-1699. doi:10.1158/1078-0432.CCR-14-0432

65. Pascual G, Avgustinova A, Mejetta S, et al. Targeting metastasis-initiating cells through the fatty acid receptor CD36. *Nature*. 2017;541(7635):41-45. doi:10.1038/nature20791

66. Pelicano H, Zhang W, Liu J, et al. Mitochondrial dysfunction in some triple-negative breast cancer cell lines: role of mTOR pathway and therapeutic potential. *Breast Cancer Res*. 2014;16(434):1-16.

67. Kim S, Lee Y, Koo JS. Differential Expression of Lipid Metabolism- Related Proteins in Different Breast Cancer Subtypes. *PLoS One*. 2015;10(3):1-15. doi:10.1371/journal.pone.0119473

68. Camarda R, Zhou AY, Kohnz RA, et al. Inhibition of fatty acid oxidation as a therapy for MYC-overexpressing triple-negative breast cancer. *Nat Med*. 2016;22(4):427-432. doi:10.1038/nm.4055

69. van Weverwijk A, Koundouros N, Iravani M, et al. Metabolic adaptability in metastatic breast cancer by AKR1B10-dependent balancing of glycolysis and fatty acid oxidation. *Nat*

Commun. 2019;10(2698):1-13. doi:10.1038/s41467-019-10592-4

70. Carracedo A, Weiss D, Leliaert AK, et al. A metabolic prosurvival role for PML in breast cancer. *J Clin Invest*. 2012;122(9):3088-3100. doi:10.1172/JCI62129

71. Wright HJ, Hou J, Xu B, Cortez M, Potma EO, Tromberg BJ. CDCP1 drives triple-negative breast cancer metastasis through reduction of lipid-droplet abundance and stimulation of fatty acid oxidation. *PNAS*. 2017;June:1-10. doi:10.1073/pnas.1703791114

72. Park JH, Vithayathil S, Kumar S, et al. Fatty Acid Oxidation-Driven Src Links Mitochondrial Energy Reprogramming and Oncogenic Properties in Triple-Negative Breast Cancer Article Fatty Acid Oxidation-Driven Src Links Mitochondrial Energy Reprogramming and Oncogenic Properties in Triple-Negative. *CellReports*. 2016;14(9):2154-2165. doi:10.1016/j.celrep.2016.02.004

73. Nath A, Chan C. Genetic alterations in fatty acid transport and metabolism genes are associated with metastatic progression and poor prognosis of human cancers. *Sci Rep*. 2016;(August 2015):1-13. doi:10.1038/srep18669

74. Lengyel E, Makowski L, Digiovanni J, Kolonin MG. Cancer as a Matter of Fat : The Crosstalk between Adipose Tissue and Tumors. *TRENDS in CANCER*. 2018;254:1-11. doi:10.1016/j.trecan.2018.03.004

75. Pascual G, Domínguez D, Benitah A. The contributions of cancer cell metabolism to metastasis. *Dis Model Mech*. 2018;11:1-11. doi:10.1242/dmm.032920

76. Nieman KM, Romero IL, Van Houten B, Lengyel E. Adipose tissue and adipocytes support tumorigenesis and metastasis. *Biochim Biophys Acta*. 2013;1831(10):1533-1541. doi:10.1016/j.bbalip.2013.02.010

77. Beloribi-Djefaflia S, Vasseur S, Guillaumond F. Lipid metabolic reprogramming in cancer cells. *Oncogenesis*. 2016;5(1):e189. doi:10.1038/oncsis.2015.49

78. Wertman J, Veinotte CJ, Dellaire G, Berman JN. The Zebrafish Xenograft Platform: Evolution of a Novel Cancer Model and Preclinical Screening Tool. In: *Advances in Experimental Medicine and Biology*. ; 2016:289-314. doi:10.1007/978-3-319-30654-4

79. White R, Rose K, Zon L. Zebrafish cancer: the state of the art and the path forward. *Nat Rev Cancer*. 2013;13(9):624-636. doi:10.1038/nrc3589

80. Letrado P, de Miguel I, Lamberto I, Díez-Martínez R, Oyarzabal J. Zebrafish: Speeding Up the Cancer Drug Discovery Process. *Cancer Res*. 2018:1-12. doi:10.1158/0008-5472.CAN-18-1029

81. Veinotte CJ, Dellaire G, Berman JN. Hooking the big one: the potential of zebrafish xenotransplantation to reform cancer drug screening in the genomic era. *Dis Model Mech*. 2014;7:745-754. doi:10.1242/dmm.015784

82. Fior R, Póvoa V, Mendes R V, et al. Single-cell functional and chemosensitive profiling of combinatorial colorectal therapy in zebrafish xenografts. *Proc Natl Acad Sci*. 2017:8234-8243. doi:10.1073/pnas.1618389114

83. Cagan RL, Zon LI, White RM. Perspective Modeling Cancer with Flies and Fish. *Dev Cell*. 2019;49(3):317-324. doi:10.1016/j.devcel.2019.04.013

84. Letrado P, Miguel I De, Lamberto I, Díez-martínez R, Oyarzabal J. Zebrafish: Speeding Up the Cancer Drug Discovery Process. *Cancer Res*. 2018;78(21):6048-6059. doi:10.1158/0008-5472.CAN-18-1029

85. White R, Rose K, Zon L. Zebrafish cancer: the state of the art and the path forward. *Nat Rev Cancer*. 2013;13(9):624-636. doi:10.1038/nrc3589

86. Zhao S, Huang J, Ye J. A fresh look at zebrafish from the perspective of cancer research. *J Exp Clin Cancer Res*. 2015;34(80):1-9. doi:10.1186/s13046-015-0196-8

87. Follain G, Osmani N, Fuchs C, Allio G, Harlepp S, Goetz JG. Chapter 15 - Using the Zebrafish Embryo to Dissect the Early Steps of the Metastasis Cascade. In: *Cell Migration: Methods and Protocols*. Vol 1749. ; 2018:195-211. doi:10.1007/978-1-4939-7701-7

88. Isogai S, Horiguchi M, Weinstein BM. The Vascular Anatomy of the Developing Zebrafish: An Atlas of Embryonic and Early Larval Development. *Dev Biol*. 2001;230:278-301. doi:10.1006/dbio.2000.9995

89. Schindelin J, Arganda-carreras I, Frise E, et al. Fiji: an open-source platform for biological-image analysis. *Nat Methods*. 2012;9(7):676-682. doi:10.1038/nmeth.2019

90. Goldsmith JR, Jobin C. Think Small: Zebrafish as a Model System of Human Pathology. *J Biomed Biotechnol*. 2012;2012:1-12. doi:10.1155/2012/817341

91. Airhart MJ, Lee DH, Wilson TD, Miller BE, Miller MN, Skalko RG. Movement disorders and neurochemical changes in zebrafish larvae after bath exposure to fluoxetine (PROZAC). *Neurotoxicol Teratol*. 2007;29:652-664. doi:10.1016/j.ntt.2007.07.005

92. Braunbeck T, Kais B, Lammer E, et al. The fish embryo test (FET): origin, applications, and future. *Environ Sci Pollut Res*. 2014;22(21):16247-16261. doi:10.1007/s11356-014-3814-7

93. Horssen R Van, Buccione R, Willemse M, Cingir S, Wieringa B, Attanasio F. Cancer cell metabolism regulates extracellular matrix degradation by invadopodia. *Eur J Cell Biol*. 2013;92(3):113-121. doi:10.1016/j.ejcb.2012.11.003

94. Cunniff B, Mckenzie AJ, Heintz NH, Howe AK. AMPK activity regulates trafficking of mitochondria to the leading edge during cell migration and matrix invasion. *Mol Biol Cell*. 2013;27(9):2662-2674. doi:10.1091/mbc.E16-05-0286

95. Caino MC, Seo JH, Aguinaldo A, et al. A neuronal network of mitochondrial dynamics regulates metastasis. *Nat Commun*. 2016;7(13730):1-11. doi:10.1038/ncomms13730

96. Novoa B, Figueras A. Zebrafish: Model for the Study of Inflammation and the Innate Immune Response to Infectious Diseases. *Adv Exp Med Biol*. 2012;946:253-275. doi:10.1007/978-1-4614-0106-3

SUPPLEMENTARY DATA

SUPPLEMENTARY FIGURES

Supplementary Figure 1 – Representation of flow cytometry histograms of MDA-MB-231^{LDL} and MDA-MB-231^{control} cells prior to xenotransplantation in zebrafish larvae. Univariate histograms of A. Bodipy; B. Cy5; C. DiI intensity in Cy5-labelled-MDA-MB-231^{LDL} (red) and DiI-labelled-MDA-MB-231^{control} (black).

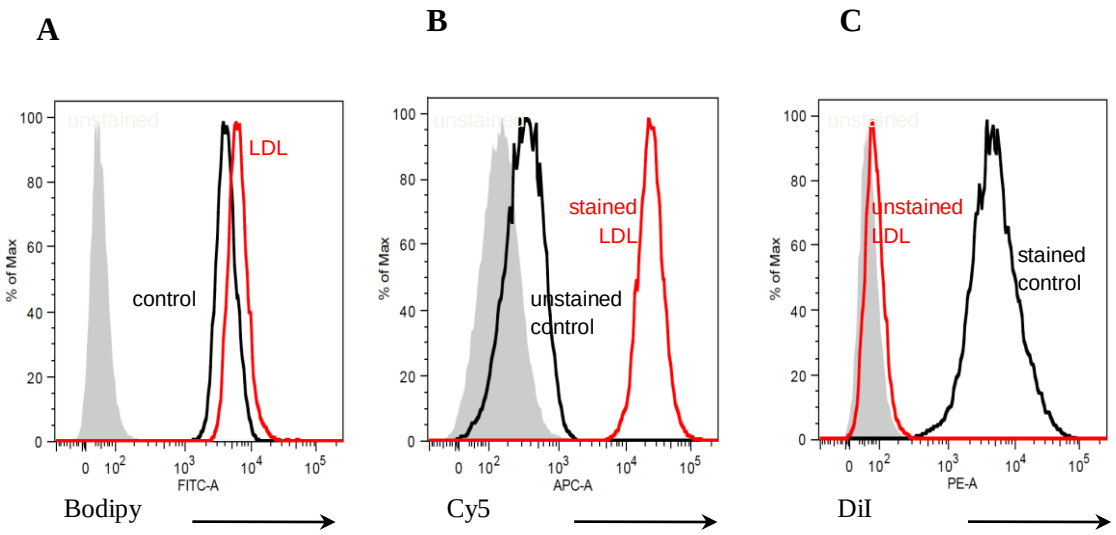

Supplementary Figure 2 – Xenotransplanted Tg (*fli1:eGFP*) zebrafish tile. Representative images of whole Tg (fli1:eGFP) zebrafish tile (4dpi and 6dpf), with organs invaded by DiI-labelled MDA-MB-231 control (red) and Cy5-labelled LDL-exposed (grey) cells and fli1 endothelial protein (green), captured with spinning disk inverted confocal microscope Zeiss Cell Observer SD. Nuclei staining with DAPI is in blue.

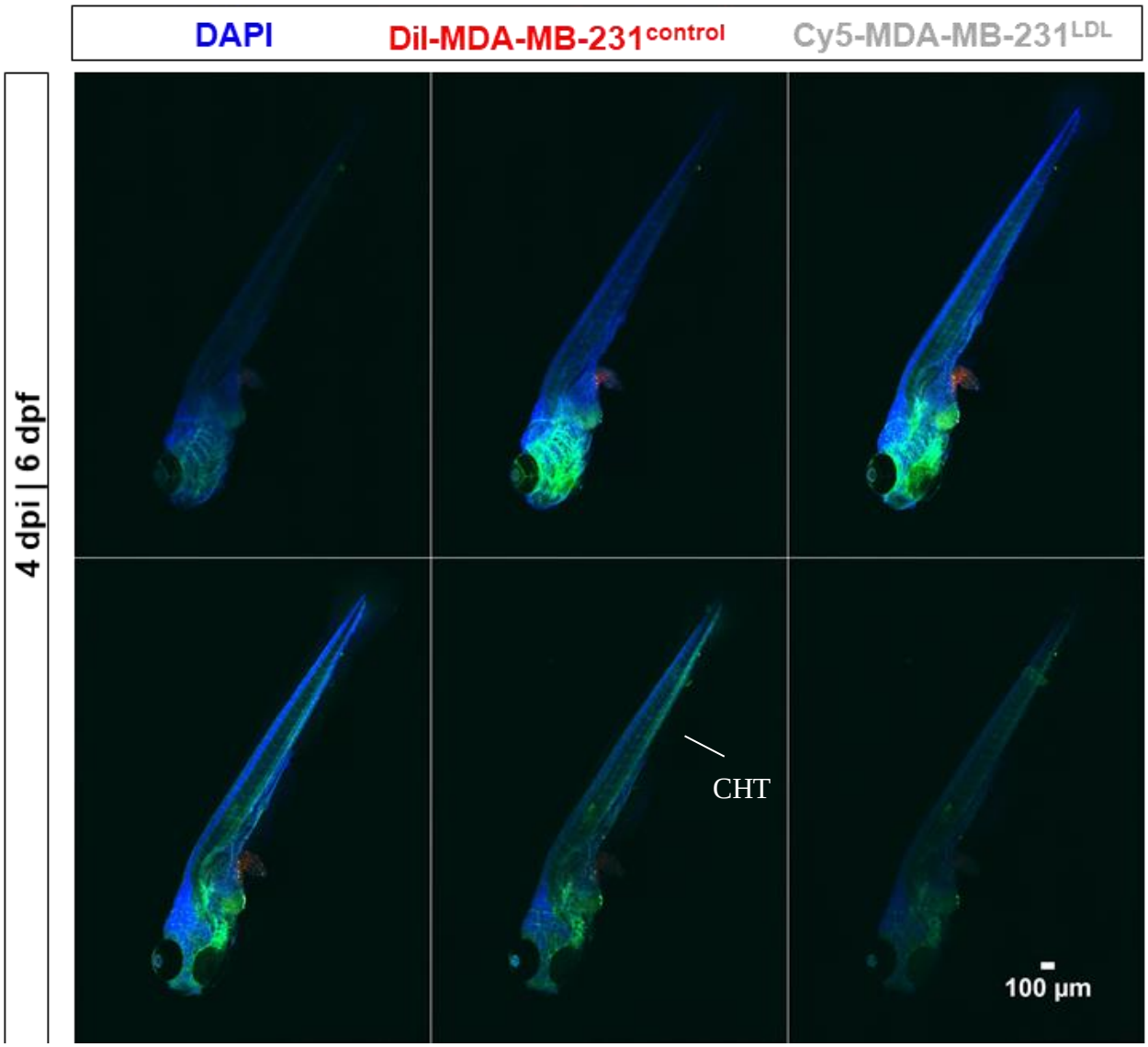

Supplementary Figure 3 – Mitochondrial Network and Cell Membrane. Binary image of maximum intensity projections of TNBC DiI-labelled MDA-MB-231 cells control (white, F); or Cy5-labelled MDA-Mb-231 (white, J) exposed to LDL, previously transfected with the mitochondrial reporter Mito-YFP (white, E and I, respectively) xenotransplanted into 2dpf zebrafish, performed with FIJI software for quantification purposes.

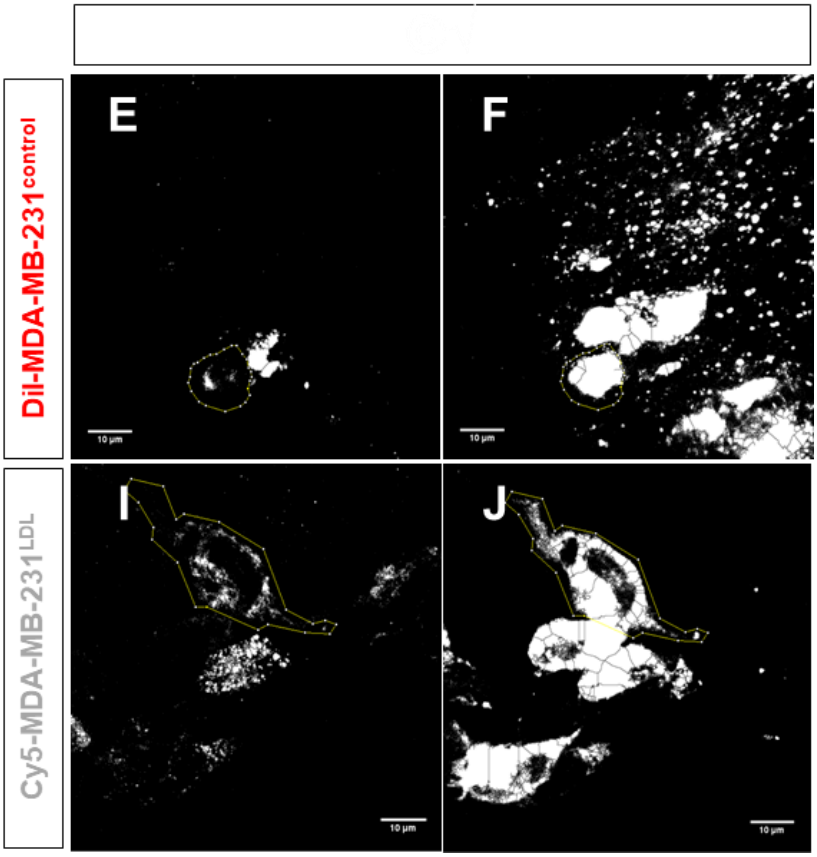

SUPPLEMENTARY TABLES

Supplementary table 1 – Tropism analysis with widefield microscopy. Binary analysis of invasion (1) or lack of invasion (0) by MDA-MB-231^{LDL} (LDL) or MDA-MB-231^{control} (control) cells in xenotransplanted zebrafish (4dpi and 6dpf) (n=25), with in the widefield microscopy.

		Eye		Brain		PVS		Swim bladder		Intestinal tract		Dorsal finn		Dorsal muscle		Notochord		Ventral muscle		Ventral finn		CHT		Anal finn		Tail fin	
		Control	LDL	Control	LDL	Control	LDL	Control	LDL	Control	LDL	Control	LDL	Control	LDL	Control	LDL	Control	LDL	Control	LDL	Control	LDL	Control	LDL	Control	LDL
Slide 1	Larvae 1			1		1	1	1		1	1		1									1					
	Larvae 2		1					1		1	1								1			1	1				1
	Larvae 3			1		1	1			1	1		1									1	1				
	Larvae 4	1	1			1	1			1	1											1	1				
	Larvae 5				1		1			1	1	1	1											1			
	Larvae 6			1	1		1		1	1	1						1					1	1	1			
Slide 2	Larvae 1					1	1			1	1				1							1					
	Larvae 2					1	1	1					1					1					1	1			
	Larvae 3						1			1						1						1	1				
	Larvae 4												1					1	1			1	1		1		
	Larvae 5					1	1				1					1				1		1					
Slide 3	Larvae 1				1	1				1	1								1	1		1					
	Larvae 2					1	1			1	1							1			1		1		1		
	Larvae 3									1	1		1				1		1			1			1		
	Larvae 4							1		1	1												1				
Slide 4	Larvae 1			1		1	1		1		1							1				1					
	Larvae 2						1				1		1				1					1	1				
	Larvae 3		1		1					1		1					1		1		1	1					
Slide 5	Larvae 1					1	1			1	1							1					1	1			1
	Larvae 2					1	1			1					1		1							1	1		
	Larvae 3					1	1			1	1							1						1			
	Larvae 4					1	1			1												1			1		
	Larvae 5			1	1	1	1			1	1			1		1					1	1		1			
	Larvae 6			1		1	1			1	1		1		1		1					1	1				
	Larvae 7		1			1	1				1						1					1	1		1		
Absolut frequency		1	4	6	5	16	19	4	2	19	19	2	8	0	5	1	8	3	9	2	3	20	16	2	11	0	1

Supplementary table 2 – Tropism analysis with spinning disk microscopy. Binary analysis of invasion (1) or lack of invasion (0) by MDA-MB-231^{LDL} (LDL) or MDA-MB-231^{control} (control) cells in xenotransplanted zebrafish (4dpi and 6dpf) (n=11), with widefield microscopy. Growth of masses, >20 cells, (1) was represented on the right of the respective cell.

		Eye		Brain		Otic vesicle		Head kidney		Liver		Heart		Gills		PVS		Swim bladder		Intestinal tract		Dorsal fin		Dorsal muscle		Notochord		Ventral muscle		Ventral fin		Orl		Anal fin		Tail fin	
		Control	LDL	Control	LDL	Control	LDL	Control	LDL	Control	LDL	Control	LDL	Control	LDL	Control	LDL	Control	LDL	Control	LDL	Control	LDL	Control	LDL	Control	LDL	Control	LDL	Control	LDL	Control	LDL	Control	LDL	Control	LDL
Slide 1	Larvae 2		1		1	1	1	1	1	1	1	1	1	1	1	1	1	1		1 1	1 1		1	1	1			1	1		1	* 1				
Slide 3	Larvae 1			1	1	1	1	1	1			1	1	1		1		1	1	1	1								1	1						
	Larvae 2					1	1	1	1	1	1	1	1	1		1	1	1	1	1	1					1				1							
	Larvae 3		1	1		1		1		1		1		1	1	1	1	1		1			1	1				1									
Slide 5	Larvae 1	1	1	1	1	1	1	1	1	1		1	1	1	1	1		1			1																
	Larvae 2		1	1	1	1	1	1	1	1		1	1	1	1	1	1	1	1	1	1		1														
	Larvae 3			1	1	1	1	1	1	1	1	1	1	1	1	1	1			1	1							1					1				
	Larvae 4		1				1		1								1 1			1	1									1							
	Larvae 5		1		1	1									1		1				1				1											
	Larvae 6		1	1		1		1		1	1	1	1	1		1	1			1			1											1			
	Larvae 7		1	1	1	1	1	1	1	1	1	1	1	1	1	1	1	1	1	1 1	1 1		1		1				1		1		1		1		
Total cell number		1	8	6	7	9	8	9	6	8	4	9	8	9	7	9	9	8	4	9	10	0	2	2	7	4	4	3	4	0	4	9	3	1	3	0	1
Total mass number		0	0	0	0	0	0	0	1	0	0	1	0	0	0	2	3	2	0	2	4	0	0	0	0	0	0	0	0	0	0	0	1	0	0	0	0

Supplementary table 3 – Invasion quantification analysis with spinning disk microscopy. Quantification of invasion by MDA-MB-231^{LDL} (LDL) or MDA-MB-231^{control} (control) cells xenotransplanted into zebrafish (4dpi and 6dpf) (n=11), with in the widefield microscopy. Growth of masses, >20 cells, (1) was represented on the right of the respective cell.

			Eye		Brain		Optic vesicle		Head kidney		Liver		Heart		Gills		PVS		Swim bladder		Intestinal tract		Dorsal fin		Dorsal muscle		Notochord		Ventral muscle		Ventral fin		Cliff		Anal fin		Tail fin	
			Control	LDL	Control	LDL	Control	LDL	Control	LDL	Control	LDL	Control	LDL	Control	LDL	Control	LDL	Control	LDL	Control	LDL	Control	LDL	Control	LDL	Control	LDL	Control	LDL	Control	LDL	Control	LDL	Control	LDL	Control	LDL
Slide 1	Larvae 2			1		2	20	1	2	2	2	1	9	2	33	3	41	38	4		106 *	80 *		1	2	1			3	1		4	54 *	2					
Slide 3	Larvae 1				1	1	5	2	10	7	6	8	10	3	1		1		3	2	33	35				1				5		1	17			1			
	Larvae 2						6	6	11	8	6	8	7	6	3		59	30	29 *	33	82	112						1					6						
	Larvae 3			4	2		15		3		2		26		19	4	60	7	1		38					1			5				22						
Slide 5	Larvae 1	2	2	1	1	1	1		3		5	0	6	7	4	1	61		2		17	8					1						8						
	Larvae 2		1	7	6		5	1	3		3		14	3	10	1	12	1	10 *	1	85	17				1		1					8						
	Larvae 3			4	1		21	4	12	3	1	2	19	14	5	3	67	44	7		25	23				1			2	1			33		4				
	Larvae 4		1					3		15								64 *				32 *								4		1						
	Larvae 5		3					3							3			*				3 *					3												
	Larvae 6		1			2	2		7		3		33 *	12	2		77 *	17			52	7			1	2							20				2		
	Larvae 7		5		3	5	3	5	20		2	3	3	3	4	5	33 *	39 *	2		65 *	79 *	0	3	3	8	0	6	10	13	0	10	180	5	1	6	0	2
Total cell number			2	18	18	18	78	25	71	50	24	14	127	50	81	20	411	240	58	47	503	396	0	3	3	8	0	6	10	13	0	10	180	5	1	6	0	2
Total mass number																	2	3	2		2	3																